

## On the Mechanism of (PCP)Ir-Catalyzed Acceptorless Dehydrogenation of Alkanes: A Combined Computational and Experimental Study

Karsten Krogh-Jespersen,\* Margaret Czerw, Nadine Summa, Kenton B. Renkema, Patrick D. Achord, and Alan S. Goldman\*

Contribution from the Department of Chemistry and Chemical Biology, Rutgers, The State University of New Jersey, New Brunswick, New Jersey 08903

Received October 31, 2001

**Abstract:** Pincer complexes of the type  $(^R\text{PCP})\text{IrH}_2$ , where  $(^R\text{PCP})\text{Ir}$  is  $[\eta^3\text{-}2,6\text{-(R}_2\text{PCH}_2)_2\text{C}_6\text{H}_3]\text{Ir}$ , are the most effective catalysts reported to date for the “acceptorless” dehydrogenation of alkanes to yield alkenes and free  $\text{H}_2$ . We calculate (DFT/B3LYP) that associative (**A**) reactions of  $(^M\text{ePCP})\text{IrH}_2$  with model linear (propane,  $n\text{-PrH}$ ) and cyclic (cyclohexane, CyH) alkanes may proceed via classical Ir(V) and nonclassical Ir(III)( $\eta^2\text{-H}_2$ ) intermediates. A dissociative (**D**) pathway proceeds via initial loss of  $\text{H}_2$ , followed by C–H addition to  $(^M\text{ePCP})\text{Ir}$ . Although a slightly higher energy barrier ( $\Delta E^\ddagger$ ) is computed for the **D** pathway, the calculated free-energy barrier ( $\Delta G^\ddagger$ ) for the **D** pathway is significantly lower than that of the **A** pathway. Under standard thermodynamic conditions (STP), C–H addition via the **D** pathway has  $\Delta G^{\circ\ddagger} = 36.3$  kcal/mol for CyH (35.1 kcal/mol for  $n\text{-PrH}$ ). However, acceptorless dehydrogenation of alkanes is thermodynamically impossible at STP. At conditions under which acceptorless dehydrogenation is thermodynamically possible (for example,  $T = 150$  °C and  $P_{\text{H}_2} = 1.0 \times 10^{-7}$  atm),  $\Delta G^\ddagger$  for C–H addition to  $(^M\text{ePCP})\text{Ir}$  (plus a molecule of free  $\text{H}_2$ ) is very low (17.5 kcal/mol for CyH, 16.7 kcal/mol for  $n\text{-PrH}$ ). Under these conditions, the rate-determining step for the **D** pathway is the loss of  $\text{H}_2$  from  $(^M\text{ePCP})\text{IrH}_2$  with  $\Delta G_{\text{D}}^\ddagger \approx \Delta H_{\text{D}}^\ddagger = 27.2$  kcal/mol. For CyH, the calculated  $\Delta G^{\circ\ddagger}$  for C–H addition to  $(^M\text{ePCP})\text{IrH}_2$  on the **A** pathway is 35.2 kcal/mol (32.7 kcal/mol for  $n\text{-PrH}$ ). At catalytic conditions, the calculated free energies of C–H addition are 31.3 and 33.7 kcal/mol for CyH and  $n\text{-PrH}$  addition, respectively. Elimination of  $\text{H}_2$  from the resulting “seven-coordinate” Ir-species must proceed with an activation enthalpy at least as large as the enthalpy change of the elimination step itself ( $\Delta H \approx 11\text{--}13$  kcal/mol), and with a small entropy of activation. The free energy of activation for  $\text{H}_2$  elimination ( $\Delta G_{\text{A}}^\ddagger$ ) is hence found to be greater than ca. 36 kcal/mol for both CyH and  $n\text{-PrH}$  under catalytic conditions. The overall free-energy barrier of the **A** pathway is calculated to be higher than that of the **D** pathway by ca. 9 kcal/mol. Reversible C–H(D) addition to  $(^R\text{PCP})\text{IrH}_2$  is predicted to lead to H/D exchange, because the barriers for hydride scrambling are extremely low in the “seven-coordinate” polyhydrides. In agreement with calculation, H/D exchange is observed experimentally for several deuteriohydrocarbons with the following order of rates:  $\text{C}_6\text{D}_6 > \text{mesitylene-}d_{12} > n\text{-decane-}d_{22} \gg \text{cyclohexane-}d_{12}$ . Because H/D exchange in cyclohexane- $d_{12}$  solution is not observed even after 1 week at 180 °C, we estimate that the experimental barrier to cyclohexane C–D addition is greater than 36.4 kcal/mol. This value is considerably greater than the experimental barrier for the full catalytic dehydrogenation cycle for cycloalkanes (ca. 31 kcal/mol). Thus, the experimental evidence, in agreement with calculation, strongly indicates that the **A** pathway is *not* kinetically viable as a segment of the “acceptorless” dehydrogenation cycle.

### Introduction

The selective catalytic functionalization of alkanes and alkyl groups remains one of the foremost challenges in the field of catalysis.<sup>1</sup> Dehydrogenation of alkanes to the corresponding olefins is a reaction of particular potential value. Significant

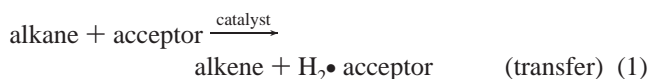
progress has been made over the past two decades toward the development of solution-phase transition-metal-based systems capable of thermally effecting this reaction.<sup>2–7</sup> Most such systems involve transfer of hydrogen to a sacrificial olefin (eq

\* To whom correspondence should be addressed. E-mail: goldman@rutchem.rutgers.edu or krogh@rutchem.rutgers.edu.

(1) For some recent reviews of homogeneously catalyzed hydrocarbon functionalization, see: (a) Arndtsen, B. A.; Bergman, R. G.; Mobley, T. A.; Peterson, T. H. *Acc. Chem. Res.* **1995**, *28*, 154–162. (b) Shilov, A. E.; Shul'pin, G. B. *Chem. Rev.* **1997**, *97*, 2879–2932. (c) Sen, A. *Acc. Chem. Res.* **1998**, *31*, 550–557. (d) Guari, Y.; Sabo-Etienne, S.; Chaudret, B. *Eur. J. Inorg. Chem.* **1999**, 1047–1055.

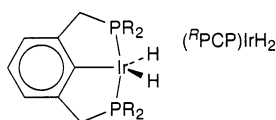
(2) (a) Baudry, D.; Ephritikine, M.; Felkin, H.; Holmes-Smith, R. *J. Chem. Soc., Chem. Commun.* **1983**, 788–789. (b) Burk, M. J.; Crabtree, R. H.; Parnell, C. P.; Uriarte, R. *J. Organometallics* **1984**, *3*, 816–817. (c) Felkin, H.; Fillebeen-Khan, T.; Gault, Y.; Holmes-Smith, R.; Zakrzewski, J. *Tetrahedron Lett.* **1984**, *25*, 1279–1282. (d) Burk, M. J.; Crabtree, R. H.; McGrath, D. V. *J. Chem. Soc., Chem. Commun.* **1985**, 1829–1830. (3) (a) Maguire, J. A.; Goldman, A. S. *J. Am. Chem. Soc.* **1991**, *113*, 6706–6708. (b) Maguire, J. A.; Petrillo, A.; Goldman, A. S. *J. Am. Chem. Soc.* **1992**, *114*, 9492–9498. (c) Wang, K.; Goldman, M. E.; Emge, T. J.; Goldman, A. S. *J. Organomet. Chem.* **1996**, *518*, 55–68.

1), but a smaller number of catalysts have been shown effective for “acceptorless” dehydrogenation (eq 2).<sup>5,7,8</sup>



Aside from the obvious and important advantage that a mole of olefin is not sacrificed, acceptorless systems are, in principle, simpler than transfer systems with respect to potential recycling and separation problems.

The family of solution-phase catalysts that have proven most effective for acceptorless dehydrogenation are those that have also been found most effective for transfer-dehydrogenation, viz., pincer catalysts of the type  $(^R\text{PCP})\text{IrH}_2$ , where  $(^R\text{PCP})\text{Ir}$  is  $[\eta^3\text{-}2,6\text{-}(\text{R}_2\text{PCH}_2)_2\text{C}_6\text{H}_3]\text{Ir}$ .<sup>4–7</sup> Transfer-dehydrogenation is more



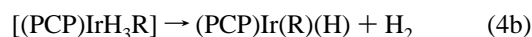
amenable to experimental mechanistic study, mainly because the acceptorless reaction must be conducted in an open system while vigorously refluxing to purge the solution of  $\text{H}_2$ . Thus, we have, to date, focused our experimental mechanistic studies on the transfer system, and we have elucidated a fairly detailed free-energy profile.<sup>9</sup> The reaction cycles of the two systems undoubtedly share several steps, including  $\beta$ -hydrogen elimination by the presumed alkyl hydride intermediates  $(\text{PCP})\text{Ir}(\text{alkyl})(\text{H})$  and subsequent loss of olefin to give  $(\text{PCP})\text{IrH}_2$ . The key difference between the acceptorless and transfer systems lies in the loss of  $\text{H}_2$  from the iridium dihydride. In the case of the transfer systems, we have shown that the dihydride loses hydrogen via insertion of the acceptor into the  $\text{Ir}-\text{H}$  bond followed by  $\text{C}-\text{H}$  elimination. Hence, an  $\text{Ir(I)}/\text{Ir(III)}$  couple is operative in accord with independent computations by Hall and by us.<sup>10,11</sup> The acceptorless system, however, must obviously lose free dihydrogen. This can, in principle, proceed either dissociatively (with  $\text{H}_2$  loss prior to alkane addition; eqs 3a,b) or associatively ( $\text{H}_2$  loss after, or concertedly with, alkane addition; eqs 4a,b). Previous computational studies have predicted that the reaction proceeds associatively, specifically via  $\text{C}-\text{H}$  oxidative addition to the dihydride:<sup>12,13</sup>



Dissociative (**D**) pathway

- (4) (a) Gupta, M.; Hagen, C.; Flesher, R. J.; Kaska, W. C.; Jensen, C. M. *Chem. Commun.* **1996**, 2083–2084. (b) Gupta, M.; Hagen, C.; Kaska, W. C.; Cramer, R. E.; Jensen, C. M. *J. Am. Chem. Soc.* **1997**, *119*, 840–841. (c) Gupta, M.; Kaska, W. C.; Jensen, C. M. *Chem. Commun.* **1997**, 461–462. (5) Xu, W.; Rosini, G. P.; Gupta, M.; Jensen, C. M.; Kaska, W. C.; Krogh-Jespersen, K.; Goldman, A. S. *Chem. Commun.* **1997**, 2273–2274. (6) Liu, F.; Pak, E. B.; Singh, B.; Jensen, C. M.; Goldman, A. S. *J. Am. Chem. Soc.* **1999**, *121*, 4086–4087. (7) Liu, F.; Goldman, A. S. *Chem. Commun.* **1999**, 655–656. (8) (a) Fujii, T.; Saito, Y. *J. Chem. Soc., Chem. Commun.* **1990**, 757–758. (b) Fujii, T.; Higashino, Y.; Saito, Y. *J. Chem. Soc., Dalton Trans.* (1972–1999) **1993**, 517–520. (c) Aoki, T.; Crabtree, R. H. *Organometallics* **1993**, *12*, 294–298.

or



Associative (**A**) pathway

In either case, the overall reaction is that shown in eq 5:



Overall reaction of eq 4 or 5; pathway unspecified

The question whether the acceptorless dehydrogenation proceeds dissociatively (**D** pathway,  $\text{Ir(I)}/\text{Ir(III)}$  couple) or associatively (**A** pathway; possibly via  $\text{Ir(V)}$ –dihydride or nonclassical  $\text{Ir(III)}$ –dihydrogen intermediates, or possibly via a concerted pathway) has relevance extending beyond this particular system.  $\text{C}-\text{H}$  bond activation by late metals is generally assumed to occur via low oxidation states and to be favored by increased electron density at the metal center. Yet, Bergman has found that cationic  $\text{Cp}^*\text{Ir(III)}$  species can add alkane  $\text{C}-\text{H}$  bonds,<sup>14</sup> and Hall has calculated that this system proceeds via an  $\text{Ir(V)}$  intermediate.<sup>15</sup> Unlike the  $(\text{PCP})\text{Ir}$  systems, an  $\text{Ir(I)}$  pathway is not accessible in the  $\text{Cp}^*\text{Ir}$  case, and the alternative of  $\sigma$ -bond-metathesis by  $\text{Cp}^*\text{Ir(III)}$  was calculated to be less favorable than the  $\text{Ir(V)}$  pathway. Further,  $\text{M(I)}/\text{M(III)}$  pathways ( $\text{M} = \text{Co}, \text{Rh}, \text{Ir}$ ) are assumed to be operative for a wide range of important reactions catalyzed by group 9 metals.<sup>16</sup> Establishing the operation of a  $\text{M(III)}/\text{M(V)}$  pathway for dehydrogenation would have obvious implications for hydrogenation with further extensions to hydroformylation, hydro-silylation, and other related catalyses.

In this paper, we confirm, experimentally and computationally, that  $\text{C}-\text{H}$  addition to the  $\text{Ir(III)}$  species can indeed occur. However, the experimental results and a detailed computational model lead firmly to the conclusion that the acceptorless dehydrogenation system does *not* operate via an associative pathway. Instead, loss of  $\text{H}_2$  occurs *dissociatively* via an  $\text{Ir(III)}/\text{Ir(I)}$  pathway. Furthermore, this dissociative loss of  $\text{H}_2$  may be the rate-determining step under the actual catalytic conditions, a result which has significant implications for any attempts at the development of related catalysts with higher turnover frequencies.<sup>17</sup>

## Results and Discussion

**Calculated Energies ( $\Delta E$ ) of  $\text{C}-\text{H}$  Addition.** Our computational modeling uses  $(^{\text{Me}}\text{PCP})$  as the basic “pincer” ligand.

- (9) Goldman, A. S.; Renkema, K. B.; Kissin, Y.; Czerw, M.; Krogh-Jespersen, K. 22nd ACS National Meeting; American Chemical Society, Washington, DC: Chicago, IL, 2001; AN 2001:637418. (10) Li, S.; Hall, M. B. *Organometallics* **2001**, *20*, 2153–2160. (11) Krogh-Jespersen, K.; Czerw, M.; Kanzelberger, M.; Goldman, A. S. *J. Chem. Inf. Comput. Sci.* **2001**, *41*, 56–63. (12) (a) Niu, S. Q.; Hall, M. B. *J. Am. Chem. Soc.* **1999**, *121*, 3992–3999. (b) Niu, S. Q.; Hall, M. B. *Chem. Rev.* **2000**, *100*, 353–405. (13) Haenel, M. W.; Oevers, S.; Angermund, K.; Kaska, W. C.; Fan, H.-J.; Hall, M. B. *Angew. Chem., Int. Ed.* **2001**, *40*, 3596–3600. (14) Klei, S. R.; Tilley, T. D.; Bergman, R. G. *J. Am. Chem. Soc.* **2000**, *122*, 1816–1817. (15) Niu, S. Q.; Hall, M. B. *J. Am. Chem. Soc.* **1998**, *120*, 6169–6170. (16) Collman, J. P.; Hegedus, L. S.; Norton, J. R.; Finke, R. G. *Principles and Applications of Organotransition Metal Chemistry*; University Science Books: Mill Valley, CA, 1987; pp 523–576. (17) Presented in part at the Pacificchem 2000 Congress, December, 2000, Honolulu; Abstract 90004907. A preliminary account of some of this work has also been communicated as ref 11.

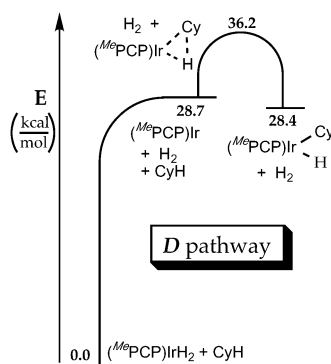


**Figure 1.** Energy profile for the dissociative pathway *D* of eq 3 (*R* = *Cy* = cyclohexyl).

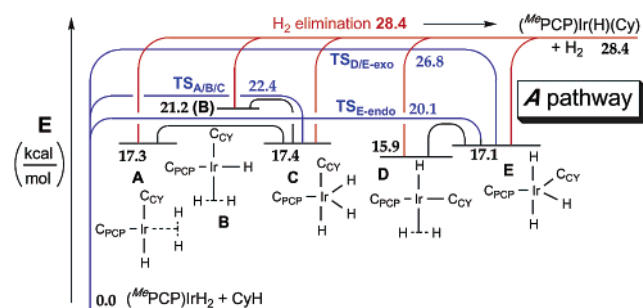


**Figure 2.** Energy profile for the associative pathway *A* of eq 4 (*R* = *Cy*). The structures of the five calculated energy minima (in the plane perpendicular to the P–Ir–P axis) are shown schematically. Pathways for C–H addition (eq 4a) are indicated by blue lines, H<sub>2</sub> elimination (eq 4b) is indicated by red lines, and interconversions of isomers are indicated by black lines.

Methyl groups on phosphorus presumably capture the electronic effects of the bulky groups used experimentally (*t*-butyl, *i*-propyl) quite well,<sup>18</sup> but in terms of exerting steric effects these may not be much better than the hydrogen atoms most often used in theoretical studies involving (model) phosphines. We will comment briefly on the Me versus *t*-Bu issue later in this report. Because most experimental studies on the (PCP)Ir-catalyzed dehydrogenation have employed cycloalkanes, we use cyclohexane (CyH) as our exemplary model substrate in the discussion; however, results for propane (*n*-PrH, 1° C–H bond), benzene, and toluene (benzylic) C–H addition are reported as well when appropriate.

The calculated value of  $\Delta E$  for loss of dihydrogen from (MePCP)IrH<sub>2</sub> (eq 3a) is 28.7 kcal/mol. Repeated attempts to locate a transition state for the dissociation were unsuccessful. The reverse reaction apparently experiences no energetic barrier in an idealized gas phase, and thus the calculated activation energy for H<sub>2</sub> loss,  $\Delta E^\ddagger$ , is also 28.7 kcal/mol. Subsequent addition of cyclohexane to three-coordinate (MePCP)Ir has a barrier of 7.5 kcal/mol. Hence, the overall reaction under study (eq 5) has a calculated  $\Delta E_D^\ddagger = 36.2$  kcal/mol for RH = CyH, when it proceeds via the dissociative pathway of eq 3 (Figure 1). The barrier to addition of *n*-PrH to (MePCP)Ir is only 6.6 kcal/mol, and eq 5 has a calculated  $\Delta E^\ddagger = 35.3$  kcal/mol.

Several configurational isomers can be envisioned as intermediates on the associative pathway (eq 4). We have located five minima with the composition (MePCP)IrH<sub>3</sub>(Cy) as indicated in Figure 2 (see Figure 3 for full structure). Some essential

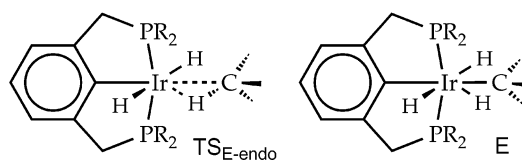


**Figure 3.** Illustration (full PCP ligand shown) of representative transition state for C–H addition via the *A* pathway (eq 4a; TS<sub>E-endo</sub>) and the corresponding addition product (intermediate *E*). See Figures 4 and 5 for a more detailed illustration of the equatorial planes of these species and of the other, isomeric, transition states and intermediates.

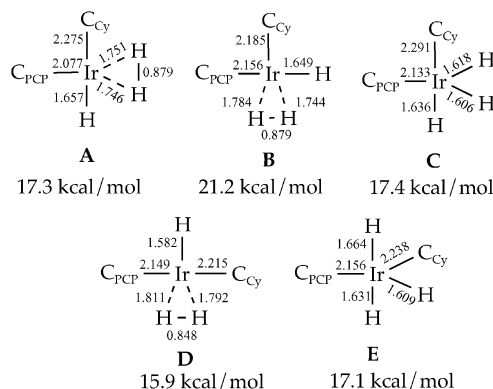


**Figure 4.** Schematic illustrations of the plane perpendicular to the P–Ir–P axis for the five minima located for C–H addition to (MePCP)IrH<sub>2</sub> (internuclear distances (Å) and energies for *R* = *Cy*). C<sub>PCP</sub> is the carbon forming the Ir–PCP linkage; C<sub>Cy</sub> is the carbon forming the Ir–Cy linkage. Ir–P bond lengths (not shown) lie in the narrow range 2.32–2.33 Å.

geometrical features associated with the coordination around the Ir metal are shown for the five minima in Figure 4.

The geometrical parameters (Figure 4) show that potential intermediates *C* and *E* are clearly classical Ir(V) C–H addition products, while intermediates *A*, *B*, and *D* are nonclassical Ir(III)( $\eta^2$ -H<sub>2</sub>) species (for convenience, we will refer to both groups of intermediates as “seven-coordinate”). Minima *A*, *C*, *D*, and *E* are almost isoenergetic, whereas minimum *B* lies ca. 4 kcal/mol higher. Importantly, interconversions among the species *A* and *C* and between the species *D* and *E* are calculated to have energy barriers that are lower ( $\leq 2$  kcal/mol) than the activation energy for the reverse reaction (C–H elimination,  $\sim 3$ –5 kcal/mol).<sup>11</sup> Furthermore, and most important later (see below), the barrier to rotation of the dihydrogen ligands around the Ir–(H<sub>2</sub>) axis is calculated to be even lower ( $\leq 1$  kcal/mol),<sup>11</sup> in accord with experimental and previously calculated values for  $\eta^2$ -H<sub>2</sub> rotation for closely related Ir(III)–dihydrogen complexes.<sup>19</sup>

Three transition states have been located for cyclohexane C–H addition (equatorial C–H bond cleavage) to (MePCP)Ir(H)<sub>2</sub>. The respective structures are shown schematically in Figure 5 (see Figure 3 for full structure of TS<sub>E-endo</sub>).

The transition state of lowest energy (TS<sub>E-endo</sub>,  $\Delta E^\ddagger = 20.1$  kcal/mol) has the cyclohexane adduct approaching the (MePCP)Ir(H)<sub>2</sub> species between the two hydrides, trans to the carbon forming the Ir–PCP linkage (C<sub>PCP</sub>), and it connects directly to minimum *E*. The transition state labeled TS<sub>A/B/C</sub> lies only 2 kcal/mol higher in energy ( $\Delta E^\ddagger = 22.4$  kcal/mol) than TS<sub>E-endo</sub>. In TS<sub>A/B/C</sub>, cyclohexane is approaching (MePCP)Ir(H)<sub>2</sub> from the

(18) van Wüllen, C. *J. Comput. Chem.* **1997**, *18*, 1985–1992.

(19) Li, S. H.; Hall, M. B.; Eckert, J.; Jensen, C. M.; Albinati, A. *J. Am. Chem. Soc.* **2000**, *122*, 2903–2910 and references therein.

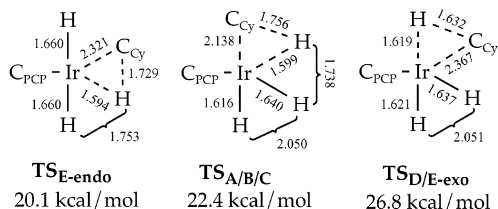


**Figure 5.** Schematic illustrations of the plane perpendicular to the P–Ir–P axis for the three transition states for C–H addition to  $(\text{MePCP})\text{IrH}_2$  (internuclear distances (Å) and energies for R = Cy). C<sub>PCP</sub> is the carbon forming the Ir–PCP linkage; C<sub>Cy</sub> is the carbon forming the Ir–Cy linkage. Ir–P bond lengths (not shown) lie in the narrow range 2.32–2.33 Å.

side (cis to C<sub>PCP</sub>), and this approach may, in principle, lead to minimum **A**, **B**, or **C**. Judging from the structural parameters of  $\text{TS}_{\text{A/B/C}}$  (Figure 5), we may anticipate that minimum **C** is the most likely product from this TS. Intrinsic reaction coordinate (IRC) calculations (see Computational and Experimental Section) were successfully employed to confirm this idea. The transition state of highest energy,  $\text{TS}_{\text{D/E-exo}}$  ( $\Delta E^\ddagger = 26.8$  kcal/mol), also has the cyclohexane approaching  $(\text{MePCP})\text{Ir}(\text{H})_2$  from the side (cis to C<sub>PCP</sub>) and could lead to minimum **D** or **E**. On the basis of its geometry and confirmed by IRC calculations,  $\text{TS}_{\text{D/E-exo}}$  actually connects to minimum **E** (as does  $\text{TS}_{\text{E-endo}}$ ). Thus, the located transition states all lead to formation of the classical “seven-coordinate” isomers (**C** and **E**). As stated above, formation of the nonclassical isomers **A** and **D** may proceed from **C** and **E**, respectively, with very low barriers. However, regardless of which C–H addition pathway is traversed, the highest energy point along the overall **A** pathway corresponds to elimination of H<sub>2</sub> from this manifold of intermediates. Because there is no barrier calculated for addition of H<sub>2</sub> to  $(\text{MePCP})\text{IrH}(\text{Cy})$ , the activation energy ( $\Delta E^\ddagger$ ) for elimination of H<sub>2</sub> from any of the minima **A–E** is equal to the thermodynamic energy difference ( $\Delta E$ ) for the elimination step (12.5 kcal/mol for RH = CyH from minimum **D**). For the overall reaction (eq 4),  $\Delta E_{\text{A}}^\ddagger = 28.4$  kcal/mol when RH = CyH ( $\Delta E_{\text{A}}^\ddagger = 28.0$  kcal/mol when RH = *n*-PrH).

It is not possible to predict which one of the two low-energy associative transition states is really the most favorable for the initial C–H addition step, because the computed energies are too similar. However, the activation energy for the associative (**A**) path,  $\Delta E_{\text{A}}^\ddagger = 28.4$  kcal/mol, is determined by the H<sub>2</sub> elimination step, and it is distinctly lower (by about 8 kcal/mol) than that calculated for the dissociative (**D**) pathway,  $\Delta E_{\text{D}}^\ddagger = 36.2$  kcal/mol. But reaction rates are of course dependent upon differences in Gibbs free energy,  $\Delta G^\ddagger = \Delta H^\ddagger - T(\Delta S^\ddagger)$ , and not on internal energy differences ( $\Delta E^\ddagger$ ).<sup>20</sup> As will be shown below, consideration of free energies leads to the conclusion that the dissociative pathway is the more favorable, even under standard thermodynamic conditions. Furthermore, the free-energy difference favoring the **D** pathway becomes quite substantial when the actual experimental conditions of the catalytic reaction (elevated temperature, low pressure of dihydrogen, bulky groups in (PCP)Ir) are carefully considered and accounted for.

(20) We use  $E$  to represent the internal purely electronic energy. The thermal electronic energy,  $E_{\text{th}}$ , may be obtained by correcting  $E$  for the effects of zero-point vibrational energies and finite temperature via the translational, rotational, and vibrational partition functions ( $E_{\text{th}} = E + E_t + E_r + E_v$ ). The enthalpy  $H$  is then  $H = E_{\text{th}} + PV = E_{\text{th}} + RT$ , and the Gibbs free energy is  $G = H - TS$ .

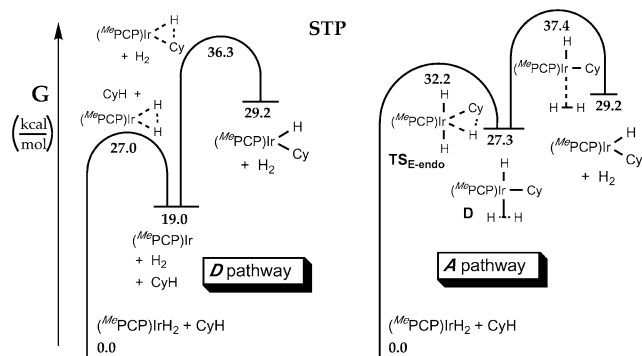


**Figure 6.** Computed free-energy profiles for **D** and **A** pathways at STP ( $T = 298$  K; all reactants and products at  $P = 1$  atm) for the reaction of cyclohexane with  $(\text{MePCP})\text{IrH}_2$ . For the **A** pathway, only the lowest-energy TS for C–H addition is shown ( $\text{TS}_{\text{E-endo}}$ ; see Figures 2–4). Likewise, only the lowest energy of the two intermediates (**D** and **E**) preceded by  $\text{TS}_{\text{E-endo}}$  is shown (see Figure 2). The TS for H<sub>2</sub> loss from either  $(\text{MePCP})\text{IrH}_2$  or **D** was not located; see ref 22 for a more detailed discussion of the estimated values.

**Calculated Gibbs Free Energies ( $\Delta G$ ) of C–H Addition: Standard Thermodynamic Conditions.** As expected, the calculated differences between  $\Delta E$  and  $\Delta H$  (or between  $\Delta E^\ddagger$  and  $\Delta H^\ddagger$ ) are generally found to be small, though they can be as much as ca. 3 kcal/mol (mostly due to the inclusion of vibrational zero-point energies in the enthalpies). However, entropic factors result in very large differences between  $\Delta H$  and  $\Delta G$  (or between  $\Delta H^\ddagger$  and  $\Delta G^\ddagger$ ).

We consider first the dissociative pathway (**D**). As stated above, there is apparently no purely electronic energy barrier for H<sub>2</sub> addition to  $(\text{MePCP})\text{Ir}$  in the gas phase (eq 3a reversed). Thus, the enthalpic barrier to H<sub>2</sub> loss may be estimated to be equal to the thermodynamic enthalpy difference for eq 3a,  $\Delta H^\ddagger$  (eq 3a)  $\approx \Delta H$  (eq 3a). Being unable to locate a conventional transition state structure from the electronic structure calculations, we cannot compute  $\Delta S^\ddagger$  for H<sub>2</sub> loss from the five-coordinate species using standard statistical mechanical expressions. However, we can estimate that the activation entropy for H<sub>2</sub> elimination must be very small on the basis of experimental data obtained on closely related “seven-coordinate” systems, that is,  $\Delta S^\ddagger$  (eq 3a)  $\approx 0$ .<sup>21</sup> Overall, the free-energy difference between  $(\text{MePCP})\text{IrH}_2$  and the TS for H<sub>2</sub> elimination,  $\Delta G^\ddagger$  (eq 3a), is thus estimated to be equal to the enthalpy difference,  $\Delta H$  (eq 3a). Under standard thermodynamic conditions ( $T = 298$  K, all reactants and products at  $P = 1$  atm), the computed value is  $\Delta H^\circ$  (eq 3a)  $\approx 27.0$  kcal/mol  $\approx \Delta G^{\circ\ddagger}$  (eq 3a).

The TS for C–H addition to  $(\text{MePCP})\text{Ir}$  (eq 3b) has a significantly higher free energy at STP than does the TS for H<sub>2</sub> loss from  $(\text{MePCP})\text{IrH}_2$  (eq 3a). Thus, the  $\Delta G^{\circ\ddagger}$  (eq 3a) value estimated above does not enter into the overall activation free-energy value for the complete **D** pathway, which is calculated to be  $\Delta G_{\text{D}}^{\circ\ddagger} = 36.3$  kcal/mol for RH = CyH at STP (Figure

(21) Activation entropies for H<sub>2</sub> loss have been determined for a series of “seven-coordinate” iridium complexes,  $(\text{PR}_3)_2\text{IrX}(\text{H})_2(\text{H}_2)$ , which are particularly closely related to the nonclassical intermediates calculated in this work. Six values were determined for  $\Delta S^\ddagger$ , ranging from  $0.7 \pm 1.0$  to  $3.7 \pm 1.1$  eu: (a) Hauger, B. E.; Gusev, D.; Caulton, K. G. *J. Am. Chem. Soc.* **1994**, *116*, 208–214. (b) Bakhtmutov, V. I.; Vorontsov, E. V.; Vymenits, A. B. *Inorg. Chem.* **1995**, *34*, 214–17. Another highly relevant study was conducted on the neutral “seven-coordinate” complexes  $\text{Ru}(\text{H})_2(\text{H}_2)(\text{PR}_3)_3$  and  $\text{Os}(\text{H})_4(\text{PR}_3)_3$ .  $\Delta S^\ddagger$  values for elimination of H<sub>2</sub> from these complexes were determined to be  $3 \pm 1$  and  $-2 \pm 4$  eu, respectively: (c) Halpern, J.; Cai, L.; Desrosiers, P. J.; Lin, Z. *J. Chem. Soc., Dalton Trans.* (1972–1999) **1991**, 717–723.

6). The computed value of  $\Delta G_D^{\circ\ddagger}$  (eq 5) includes an overall value of  $\Delta S_D^{\circ\ddagger} \approx -13$  eu relative to the reactants ( $(^{\text{Me}}\text{PCP})\text{-IrH}_2 + \text{CyH}$ ), reflecting the sum of the favorable entropy attributable to the elimination of a free  $\text{H}_2$  molecule (26.8 eu at 1 atm  $\text{H}_2$ ) and the quite unfavorable entropic contribution of the C–H addition step ( $\sim -40$  eu). The computed activation entropy for C–H elimination from  $(^{\text{Me}}\text{PCP})\text{Ir}(\text{Cy})(\text{H})$  is only  $\Delta S^{\circ\ddagger}$  (eq 3b) = 0.3 eu, a very small value which provides some additional support for the estimate  $\Delta S^{\circ\ddagger}$  (eq 3a)  $\approx 0$  for  $\text{H}_2$  loss from  $(^{\text{Me}}\text{PCP})\text{IrH}_2$  made above. Apparently, the entropic gain associated with the group ( $\text{H}_2$  or  $\text{CyH}$ ) leaving the (PCP)-Ir species is not realized until after the transition state has been reached.

Turning now to the associative pathway (eq 4), we find, as expected, that  $\Delta S^{\circ\ddagger}$  for C–H addition is significantly negative, about  $-46$  to  $-48$  eu. The large difference between this value and that for C–H addition via the dissociative pathway ( $\Delta S^{\circ\ddagger} \approx -13$  eu) reflects the absence of a free molecule of  $\text{H}_2$  in the *A* pathway and a small additional contribution of ca.  $-7$  eu resulting from the greater steric crowding in the TS for C–H addition to  $(^{\text{Me}}\text{PCP})\text{IrH}_2$  as compared with addition to  $(^{\text{Me}}\text{PCP})\text{-Ir}$ . Factoring in the very negative entropy terms for C–H addition via the *A* pathway produces large free energies of activation. The TS of lowest free energy for C–H addition via the *A* pathway (eq 4a) is calculated to be 32.2 kcal/mol for cyclohexane ( $\text{TS}_{\text{E-endo}}$ ). This value is substantial, but the TS for loss of  $\text{H}_2$  (eq 4b) from the resulting “seven-coordinate” adducts (**D/E**) has an even higher enthalpy – *even if it is assumed to be no higher in enthalpy than the reaction product, that is, the alkyl hydride*. A barrier for addition of  $\text{H}_2$  to  $(^{\text{Me}}\text{PCP})\text{-Ir}(\text{Cy})\text{H}$  cannot be found on the potential energy surface, and it is thus not possible to directly calculate the entropy or free energy of the transition state for  $\text{H}_2$  elimination ( $\text{TS}_{\text{H}_2\text{elim}}$ ) from the “seven-coordinate” intermediate. In analogy to the considerations made above, we assume that  $\text{TS}_{\text{H}_2\text{elim}}$  from **D/E** has entropy similar to that of either intermediate **D** or  $\text{TS}_{\text{E-endo}}$  (the TS for C–H elimination from **D/E**) and obtain a free energy of activation  $\Delta G^{\circ\ddagger} = 37.4$  kcal/mol for  $\text{H}_2$  elimination.<sup>21,22</sup> Therefore, this step (eq 4b) is apparently rate-determining for the *A* pathway on the potential energy surface (Figure 2) as well as on the Gibbs free-energy surface (Figure 6).

It is worth noting that the value of  $\Delta G_A^{\circ\ddagger}$  obtained above, 37.4 kcal/mol for eq 5 (RH = CyH), is derived from calculations which indicate that no point along the *A* pathway is of higher enthalpy than the products,  $(^{\text{Me}}\text{PCP})\text{IrRH} + \text{H}_2$ . Nevertheless,  $\Delta G_A^{\circ\ddagger}$  is quite high due to the combination of the high (thermodynamic) reaction enthalpy of eq 5 (25.3 kcal/mol for R = Cy; 24.9 kcal/mol for R = *n*-Pr) and the substantial unfavorable entropic contribution. Because the entropic contribution is essentially unavoidable in *any* bimolecular pathway,<sup>21</sup> the value thus obtained for  $\Delta G_A^{\circ\ddagger}$  may be regarded as a quite reliable lower limit.<sup>21,23</sup> This barrier ( $\Delta G_A^{\circ\ddagger} = 37.4$  kcal/mol) is found to be ca. 1 kcal/mol higher than  $\Delta G_D^{\circ\ddagger}$ , and it is ca. 5

kcal/mol higher than the barrier to the prior C–H addition step (eq 4a) in the *A* pathway.

**Calculated Gibbs Free Energies ( $\Delta G$ ) of C–H Addition: Experimental Conditions.** As just noted, under standard thermodynamic conditions,  $\Delta G^{\circ\ddagger}$  is calculated to be slightly *lower* for the *D* pathway than for the *A* pathway. The *D* pathway would thus be predicted to be operative, but the computed difference in free energies is so small ( $\sim 1$  kcal/mol) that it is certainly testing the confidence limits of the calculations. However, the actual catalytic reaction certainly is not (and cannot be) conducted under standard conditions (298 K, 1 atm in all reactants and products).  $\Delta G^\circ$  of alkane dehydrogenation is highly positive under 1 atm  $\text{H}_2$  ( $\sim 16$  kcal/mol), and an extremely low steady-state concentration of  $\text{H}_2$  (less than the equilibrium concentration value for eq 2) must be maintained in solution or the reaction (eq 2) will proceed to the left, rather than to the right. Furthermore, the high reaction endothermicity inevitably requires elevated temperatures, which also help favor the reaction thermodynamics; in no case has acceptorless dehydrogenation been reported at temperatures below 151 °C (and at that temperature only for the “easily” dehydrogenated substrate cyclooctane).<sup>5,7,8,24–26</sup>

Clearly, to obtain free-energy parameters computationally that are relevant to experiment, it will be necessary to model the reactions as closely as possible to experimental conditions. From the thermodynamic literature, the maximum steady-state concentration of  $\text{H}_2$  required for alkane dehydrogenation to produce significant yield of olefin can be calculated to correspond to a  $\text{H}_2$  pressure of ca.  $10^{-14}$  atm at 25 °C. At the elevated temperatures of the actual experiments, more relevant values are ca.  $1.0 \times 10^{-7}$  atm at 150 °C and ca.  $1.0 \times 10^{-5}$  atm at 200 °C.<sup>25–27</sup> We have used these two temperature/pressure combinations to calculate free-energy profiles for each of the hydrocarbon substrates that we have studied (Table 1).

It should be noted that any calculated differences in  $\Delta G$  and  $\Delta G^\ddagger$  resulting from the application of a nonstandard pressure of dihydrogen are completely rigorous in terms of fundamental thermodynamic laws. They follow from the simple relationship for the pressure dependence of the chemical potential for a species X:

$$\mu_X = \mu_X^\circ + RT[\ln(P_X/P_X^\circ)] \quad (6)$$

(22) If we assume that the entropy of the transition state for  $\text{H}_2$  elimination,  $\text{TS}_{\text{H}_2\text{elim}}$ , is the same as that of intermediate **D**, we can estimate the free-energy difference on the basis of the enthalpy difference between the two states, which gives a value of 36.0 kcal/mol for  $\text{TS}_{\text{H}_2\text{elim}}$ . The transition state for C–H elimination,  $\text{TS}_{\text{E-endo}}$ , presents an alternative model for the entropy of  $\text{TS}_{\text{H}_2\text{elim}}$ . Extrapolating from the enthalpy difference in this case gives a free energy of 38.8 kcal/mol. The average of these two values, 37.4 kcal/mol, is shown in Figure 7. The basis for this estimation method is well established, particularly for related “seven-coordinate” iridium complexes (see ref 21).

(23) Determination of the thermodynamics for reaction 5 involves the comparison of two very similar species, that is,  $(\text{PCP})\text{Ir}(\text{R})(\text{H})$  and  $(\text{PCP})\text{Ir}(\text{H})_2$ . Electronic structure calculations (DFT or otherwise) are well known to give highly reliable results, when comparisons of similar species are made. It is worth noting that our values for the thermodynamics of this reaction are in good agreement with related calculations by Hall (refs 12 and 13), and they have been calibrated and found to be quite accurate for the observable species (*t*-BuPCP)IrH<sub>2</sub> and (*t*-BuPCP)Ir(Ph)H (ref 9).

(24) The dehydrogenation enthalpy of cyclooctane is approximately 23.8(5) kcal/mol as determined by either direct measurement of hydrogenation or on the basis of enthalpies of formation.<sup>25,26</sup> This can be compared, for example, with the following enthalpies (kcal/mol) for the formation of alkenes from *n*-butane: *trans*-2-butene, 27.5; *cis*-2-butene, 28.5; 1-butene, 30.1.<sup>25,26</sup>

(25) NIST Standard Reference Database Number 69, 1996, <http://webbook.nist.gov/chemistry/>.

(26) Stull, D. R.; Westrum, E. F.; Sinke, G. C. *The Chemical Thermodynamics of Organic Compounds*; Robert E. Kreiger Publishing: Malabar, FL, 1987.

(27) For example, for the dehydrogenation of *n*-hexane(liq) to give 1-hexene and *trans*-2-hexene, the values of  $\Delta G$  at 25 °C are 20.97 and 18.37 kcal/mol, respectively.<sup>25</sup> At 1.0 M hexene and 10 M *n*-hexane, the equilibrium pressures of  $\text{H}_2$  at 25 °C are thus  $4.2 \times 10^{-15}$  and  $3.4 \times 10^{-13}$  atm, respectively. At 150 °C, the respective pressures are  $1.5 \times 10^{-8}$  and  $3.4 \times 10^{-7}$  atm. At 200 °C, the respective pressures are  $6.8 \times 10^{-7}$  and  $1.1 \times 10^{-5}$  atm. Throughout the course of this work, we use  $1.0 \times 10^{-7}$  atm at 150 °C and  $1.0 \times 10^{-5}$  atm at 200 °C.

**Table 1.** Calculated Free Energies of Activation for **A** and **D** Pathways (H<sub>2</sub> Elimination and C–H Addition), and Free Energies of Lowest Intermediate for the **A** Pathway

hydrocarbon	<i>T</i> (°C)	<i>P</i> <sub>H<sub>2</sub></sub> (atm) <sup>a</sup>	<i>D</i> path		<i>A</i> path		
			H <sub>2</sub> diss <sup>b</sup>	C–H add <sup>c</sup>	C–H add <sup>d</sup>	IrH <sub>3</sub> R <sup>e</sup>	H <sub>2</sub> elim <sup>f</sup>
benzene	25	STP	27.0	25.4	25.2	14.9	27.9
benzene	150	10 <sup>−7</sup>	27.2	7.1	24.6	14.2	27.7
benzene	200	10 <sup>−5</sup>	27.3	9.7	26.1	15.6	29.2
toluene	25	STP	27.0	31.5	29.1	20.5	33.2
toluene	150	10 <sup>−7</sup>	27.2	13.7	28.9	20.2	33.3
toluene	200	10 <sup>−5</sup>	27.3	16.5	30.6	21.9	35.1
propane	25	STP	27.0	35.1	32.7	26.3	37.7
propane	150	10 <sup>−7</sup>	27.2	16.7	33.7	25.5	36.6
propane	200	10 <sup>−5</sup>	27.3	19.2	35.2	26.9	38.1
cyclohexane	25	STP	27.0	36.3	32.2	27.3	37.4
cyclohexane	150	10 <sup>−7</sup>	27.2	17.5	31.3	25.6	36.0
cyclohexane	200	10 <sup>−5</sup>	27.3	20.0	32.8	26.8	37.3

<sup>a</sup> At STP, *P* = 1 atm for all reactants and products. At other conditions, *P*<sub>H<sub>2</sub></sub> is the value given, and a value of *P*<sub>RH</sub> is used to give the density of C–H bonds in solution of the corresponding hydrocarbon (see text for discussion). <sup>b</sup> Estimated free energy of activation for loss of H<sub>2</sub> from (MePCP)IrH<sub>2</sub>, equal to the enthalpy of H<sub>2</sub> loss (see ref 21 and text for discussion). <sup>c</sup> Free energy (relative to (MePCP)IrH<sub>2</sub> plus RH) of the TS for R–H addition to (MePCP)Ir plus a free molecule of H<sub>2</sub>. <sup>d</sup> Δ*G*<sup>‡</sup> of C–H addition to (MePCP)IrH<sub>2</sub> for the TS of lowest energy. <sup>e</sup> Free energy (relative to (MePCP)IrH<sub>2</sub> plus RH) of the lowest energy intermediate (with stoichiometry [(MePCP)IrH<sub>3</sub>R]) preceded by the lowest energy TS for C–H addition to (MePCP)IrH<sub>2</sub>. <sup>f</sup> Estimated free energy (relative to (MePCP)IrH<sub>2</sub> plus RH) of the “TS” for H<sub>2</sub> elimination via the associative path. The value is assumed to have an enthalpy no higher than the enthalpy of the products. The entropy is then estimated as an average of the entropy value calculated for the preceding intermediate ((MePCP)IrH<sub>3</sub>R]) and that for the preceding TS for C–H addition/elimination (see ref 21 and text for discussion).

Thus, for example, for a state that includes free H<sub>2</sub>, the use of *P*<sub>H<sub>2</sub></sub> = 1.0 × 10<sup>−7</sup> atm instead of 1.0 atm results in a free-energy change equal to *T*(*R* ln 10<sup>−7</sup>) or, equivalently, an entropy change of *R* ln 10<sup>−7</sup> ≈ 32.0 eu.

We should also include statistical terms to account for the increased density of C–H bonds in alkane solution vis-à-vis gas phase at 1 atm. Neat alkane solvent has a concentration of ca. 10 mol/L (e.g., 9.3 mol/L for cyclohexane), whereas the standard calculations assume 1 atm (~0.041 mol/L at STP). The gas–liquid concentration correction is equivalent to an entropy correction of *R* ln(10/0.041). Finally, because the basic statistical mechanical expressions only take into account a single C–H bond of the hydrocarbon, we must also correct for the statistically greater number of C–H bonds available per molecule that may add to iridium. Thus, when the addendum is cyclohexane (12 C–H bonds), we include an overall C–H bond density factor of *R* ln[12 × (10/0.041)]. Although this entropic correction is less rigorous than the one used for the dihydrogen pressure, it is also less important in the context of differentiating between the **A** and **D** pathways. For both pathways, the respective C–H addition transition states are favored by the same factor, which thus cancels out in evaluating the difference between these two transition states.

In the case of the *dissociative* pathway (**D**), the use of experimental temperature and hydrogen pressure conditions results in a significantly lower calculated value of Δ*G*<sup>‡</sup> for C–H addition, because the relevant transition state includes a molecule of free H<sub>2</sub>. When compared with data obtained at STP, the use of *P*<sub>H<sub>2</sub></sub> = 1.0 × 10<sup>−7</sup> atm and *T* = 150 °C (423 K) results in a decrease of 12.7 kcal/mol for Δ*G*<sup>‡</sup>. The entropic factor accounting for the density of C–H bonds yields a further decrease of 6.7 kcal/mol (cyclohexane). As a result of these corrections (plus

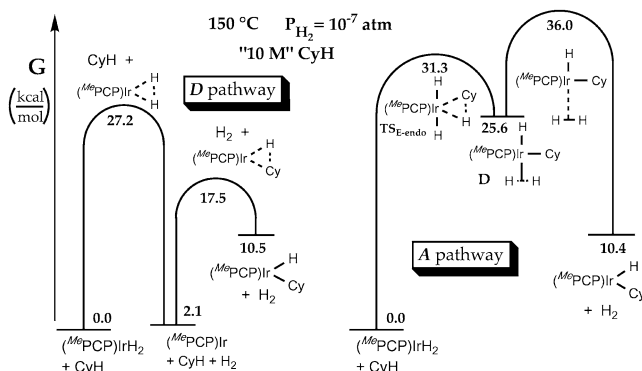


**Figure 7.** Free-energy profiles for **D** and **A** pathways at *T* = 150 °C, *P*<sub>H<sub>2</sub></sub> = 10<sup>−7</sup> atm, and [cyclohexane] = 10 mol/L for the reaction of cyclohexane with (MePCP)IrH<sub>2</sub>. See caption, Figure 6, for details. Note that, under these conditions (in contrast with STP; Figure 6), the rate-determining step for the **D** pathway is loss of H<sub>2</sub>, not C–H addition.

small changes due to the temperature-dependence of Δ*H*<sup>‡</sup>, the TS for C–H addition to (MePCP)Ir (eq 3b) is calculated to be at a much lower free energy under “experimental” conditions (17.5 kcal/mol, relative to (MePCP)IrH<sub>2</sub> and cyclohexane) than is the TS for H<sub>2</sub> loss (eq 3a; 27.2 kcal/mol, see Figure 7). We conclude that under conditions where acceptorless dehydrogenation (eq 2) is experimentally possible, the rate-determining step for the **D** pathway is elimination of H<sub>2</sub> (eq 3a, rather than eq 3b) with Δ*G*<sub>D</sub><sup>‡</sup> = 27.2 kcal/mol.

The **A** pathway is also favored by 6.7 kcal/mol from the higher solution density of cyclohexane C–H bonds. However, as compared with results obtained at STP, this factor is offset (almost exactly, by coincidence) by the higher temperature (150 °C) which disfavors the entropically unfavorable addition reaction. At 150 °C, the computed value of Δ*G*<sup>‡</sup> for eq 4a (RH = CyH) is 31.3 kcal/mol. The TS for H<sub>2</sub> loss from the resulting “seven-coordinate” species has an even higher free energy of 36.0 kcal/mol, relative to the iridium–dihydride and cyclohexane (Figure 7). Thus, the computed Δ*G*<sub>A</sub><sup>‡</sup> is 36.0 kcal/mol for eq 5 (RH = CyH), and the calculated difference between the overall free-energy barriers of the two pathways, ΔΔ*G*<sub>A/D</sub><sup>‡</sup>, is substantial, 8.8 kcal/mol for RH = CyH, and is unequivocally *in favor* of the **D** pathway. Analogous calculations give a similar value for propane (1° C–H), ΔΔ*G*<sub>A/D</sub><sup>‡</sup> = 36.6 – 27.2 = 9.4 kcal/mol (favoring **D**; Table 1).

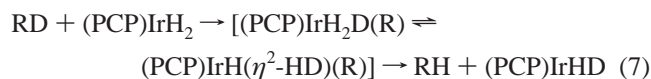
**Bulky Alkyl Groups.** It is noteworthy that the very large calculated preference for the **D** pathway results even though the calculations are conducted using methyl groups, rather than *t*-butyl or *i*-propyl groups, on the PCP phosphorus atoms. Bulkier alkyl (or aryl) groups would undoubtedly serve to further increase the free energy of the crowded transition states encountered on the **A** pathway. Even if the TS for C–H addition to (R<sup>3</sup>PCP)Ir (i.e., the second step in the **D** pathway) could be equally disfavored by steric factors, which seems highly unlikely because it is less crowded than the TS for C–H addition to (R<sup>3</sup>PCP)IrH<sub>2</sub>, this would have no effect on the overall Δ*G*<sub>D</sub><sup>‡</sup> until steric factors become so severe that C–H addition (eq 3b) rather than H<sub>2</sub> loss becomes rate-determining for the **D** pathway. This would require ca. 10 kcal/mol of additional steric repulsion in the case of RH = CyH (Figure 7). Adding this magnitude of steric energy to the free energies of *both* **A** and **D** transition states for C–H addition would increase the value of ΔΔ*G*<sub>A/D</sub><sup>‡</sup> to approximately 19 kcal/mol in favor of the **D** pathway for

**Table 2.** Thermodynamic and Activation Enthalpies and Entropies of the Relevant Addition Reactions at STP

addendum	Ir species	$\Delta H^\ddagger$	$\Delta H$	$\Delta S^\ddagger$	$\Delta S$	$\Delta G^\ddagger$	$\Delta G$
H <sub>2</sub>	( <sup>Me</sup> PCP)Ir	0.0	-27.0	-26.8	-26.8	8.0	-19.0
benzene	( <sup>Me</sup> PCP)Ir	-5.4	-12.3	-39.1	-30.6	6.3	-3.2
toluene	( <sup>Me</sup> PCP)Ir	0.9	-7.5	-45.2	-43.3	12.5	4.3
propane(1°)	( <sup>Me</sup> PCP)Ir	4.7	-2.2	-38.0	-37.0	16.0	8.8
cyclohexane	( <sup>Me</sup> PCP)Ir	5.4	-1.7	-39.8	-40.0	17.2	10.2
benzene	( <sup>Me</sup> PCP)IrH <sub>2</sub>	13.2	1.7	-44.8	-44.7	25.2	15.0
toluene	( <sup>Me</sup> PCP)IrH <sub>2</sub>	14.3	5.7	-50.0	-49.8	29.1	20.5
propane(1°)	( <sup>Me</sup> PCP)IrH <sub>2</sub>	19.4	13.5	-44.8	-43.0	32.7	26.3
cyclohexane	( <sup>Me</sup> PCP)IrH <sub>2</sub>	18.4	15.1	-46.5	-40.8	32.2	27.3

either cyclohexane (see Figure 7) or propane. Any additional steric repulsion, if it affected the **A** and the **D** transition states equally, would not change this very substantial value.

**Experimental Determination of the Barrier to the A Pathway: H/D Exchange.** The calculations clearly predict that the **A** pathway has a much greater barrier than the **D** pathway (for eq 5). Furthermore, a considerably greater barrier is predicted for the **A** pathway (36.0 kcal/mol for cyclohexane and (<sup>Me</sup>PCP)IrH<sub>2</sub> at 150 °C) than is experimentally observed for the actual, overall, catalytic reactions (for example, 30.0 kcal/mol for cyclooctane and (<sup>t-Bu</sup>PCP)IrH<sub>2</sub> at 150 °C). The problem of experimentally testing the conclusions of these calculations is quite intriguing. The reaction in question (eq 5) yields an intermediate, which has never been observed when RH = alkane; indeed, formation of the alkyl hydrides (with loss of H<sub>2</sub>) is calculated to be endothermic, and, in addition, the alkyl hydrides are presumably subject to relatively rapid  $\beta$ -hydrogen elimination. Even for an observable model species, such as (<sup>t-Bu</sup>PCP)Ir(Ph)(H),<sup>28</sup> eq 5 is highly endothermic (calculated  $\Delta H = -12.3 - (-27.0) = 14.7$  kcal/mol; Table 2), which effectively precludes kinetic measurements. Thus, direct measurement of the barrier of eq 5 seems a formidable task. However, the nature of the associative pathway, irrespective of the calculated values of  $\Delta G^\ddagger$ , suggests a way to determine at least an upper limit to its rate. Because the calculated associative pathway involves intermediate nonclassical dihydrogen complexes, or intermediates that are in rapid equilibrium with dihydrogen complexes, (PCP)IrH<sub>2</sub> should undergo H/D exchange with a deuteriohydrocarbon solvent at a rate at least comparable to that of the associative reaction.



Note that actual observation of H/D exchange (eq 7) does not demonstrate that a full associative exchange has occurred (eq 5), because the step after C–H addition (i.e., H<sub>2</sub> or HD elimination from the adduct) may not necessarily have taken place. In fact, as noted above, the calculations suggest that the barrier to loss of H<sub>2</sub> from the “seven-coordinate” alkane C–H addition products (eq 4b) is higher than that for C–H addition/elimination, eq 4a (see Figures 6 and 7), though the small differences are perhaps within the uncertainty level of the calculations. Thus, the rate of H/D exchange (eq 7) should provide a good *upper limit* estimate to the rate of associative exchange (eq 5); that is,  $\Delta G_7^\ddagger$  provides a lower limit for  $\Delta G_5^\ddagger$ . If H<sub>2</sub> elimination from the C–H adduct (eq 4b) is indeed slower

**Scheme 1.** General Reaction Scheme Used for Kinetic Modeling To Obtain the Rate of H/D Exchange between Deuteriohydrocarbons and (<sup>t-Bu</sup>PCP-*d<sub>n</sub>*)IrH<sub>2</sub> (See Experimental Section for Details)



than C–H elimination (eq 4a, reverse), then the rate of H/D exchange will be faster than the rate of eq 5.

The addition of benzene to (<sup>Me</sup>PCP)Ir is calculated to be much more thermodynamically favorable than addition of alkanes (see Table 2); accordingly, the corresponding substitution of H<sub>2</sub> by R–H (eq 5) is thermodynamically much more favorable for benzene. Addition of RH to (<sup>Me</sup>PCP)IrH<sub>2</sub> to produce the (<sup>Me</sup>PCP)IrH<sub>3</sub>R intermediate is also thermodynamically more favorable for benzene (by 13.4 kcal/mol) than for cyclohexane, and the associative transition state for benzene addition (25 °C) is calculated to be 5.2 kcal/mol lower than that for cyclohexane. These results are in accord with all previous experimental comparisons revealing that addition of benzene to late metal centers is both kinetically and thermodynamically much more favorable than addition of alkanes.<sup>29</sup> The barrier ( $\Delta G^\ddagger$ ) for benzene addition to (<sup>Me</sup>PCP)IrH<sub>2</sub> is calculated to be 24.6 kcal/mol, when corrections are applied for the C–H bond concentration of neat benzene. The reverse reaction (elimination of benzene from the lowest energy intermediate, minimum **A** in this case (see Figure 2)) has a barrier of ca. 11.8 kcal/mol, which is substantially greater than the barrier calculated for rotation of H<sub>2</sub>.<sup>19</sup> Thus, H/D exchange between C<sub>6</sub>D<sub>6</sub> and (<sup>Me</sup>PCP)IrH<sub>2</sub> is calculated to occur with a barrier of  $\Delta G^\ddagger = 25.2$  kcal/mol at 25 °C ( $\Delta G^\ddagger = 20.9$  kcal/mol when the concentration of C–H bonds in neat benzene is taken into account) before adjustments are made for isotope effects and for statistical terms that would account for nonproductive addition/elimination.

Experimentally, H/D exchange is observed to occur between C<sub>6</sub>D<sub>6</sub> and (<sup>t-Bu</sup>PCP)IrH<sub>2</sub>. The kinetic analysis of the data is slightly complicated by incorporation of deuterium into the *t*-butyl groups. The concentration of C<sub>6</sub>D<sub>5</sub>H, (<sup>t-Bu</sup>PCP-*d<sub>n</sub>*)IrH<sub>2</sub>, (<sup>t-Bu</sup>PCP-*d<sub>n</sub>*)IrHD, as well as the total fraction of protium in the PCP *t*-butyl groups, was monitored over time by <sup>1</sup>H NMR. Fortunately, there is no exchange with the <sup>t-Bu</sup>PCP methylene groups, which provide a good integration standard for the determination of percent-deuteration at the hydride and *t*-butyl positions. Also fortunate is the fact that the dihydride and the mixed hydride-deuteride signals are easily resolved in the hydride region of the <sup>1</sup>H NMR spectrum. Analysis by kinetics simulation programs gives a best fit to all of the species monitored with a rate constant for eq 7 of  $k_{\text{RD/IrH}} = 6 \times 10^{-5} \text{ M}^{-1} \text{ s}^{-1}$ . A simplified reaction scheme for the fit is shown in Scheme 1; see Experimental Section for details. The fit is insensitive to the value of  $k_{\text{t-Bu/IrD}}$  as long as the value used is much larger than  $k_{\text{RD/IrH}}$ .

(28) Kanzelberger, M.; Singh, B.; Czerw, M.; Krogh-Jespersen, K.; Goldman, A. S. *J. Am. Chem. Soc.* **2000**, *122*, 11017–11018.

(29) For reviews of alkane C–H bond activation by organometallic complexes, see ref 1 and (a) Jones, W. D.; Feher, F. J. *Acc. Chem. Res.* **1989**, *22*, 91–100. (b) Crabtree, R. H. *Chem. Rev.* **1985**, *85*, 245. (c) Halpern, J. *Inorg. Chim. Acta* **1985**, *100*, 41–48. Some more recent papers that have addressed selectivity in particular and provide good lead references include: (d) Harper, T. G. P.; Desrosiers, P. J.; Flood, T. C. *Organometallics* **1990**, *9*, 2523–2528. (e) Bennett, J. L.; Vaid, T. P.; Wolczanski, P. T. *Inorg. Chim. Acta* **1998**, *270(1–2)*, 414–423. (f) Wick, D. D.; Jones, W. D. *Organometallics* **1999**, *18*, 495–505. (g) McNamara, B. K.; Yeston, J. S.; Bergman, R. G.; Moore, C. B. *J. Am. Chem. Soc.* **1999**, *121*, 6437–6443.

**Table 3.** Experimental Rates and Free Energies of H/D Exchange (Eq 7,  $k_{RD/IRH}$  Extrapolated from Scheme 1), and Corresponding Calculated  $\Delta G^\ddagger$  Values of C–H Addition to  $(^{Me}PCP)IrH_2$  (Eq 4a)<sup>a</sup>

calculated ( $^{Me}PCP$ )IrH <sub>2</sub>			experimental ( $^{t-Bu}PCP$ )IrH <sub>2</sub>				
R–H	$\Delta G_{4a}^\ddagger$ (kcal/mol)		R–H	T (°C)	$k_{7(extrap)}$ (M <sup>-1</sup> s <sup>-1</sup> )	rate <sub>7a</sub> (s <sup>-1</sup> )	$\Delta G_{7a(extrap)}^\ddagger$ (kcal/mol)
benzene	20.9 at 25 °C (21.1 at 30 °C)		benzene	30	$1.2 \times 10^{-4}$	$2.8 \times 10^{-3}$	21.3
toluene	23.5 at 25 °C (27.5 at 110 °C)		mesitylene	110	$7.2 \times 10^{-5}$	$1.0 \times 10^{-3}$	27.9
C <sub>3</sub> H <sub>7</sub> –H(1°)	29.1 at 25 °C (32.3 at 130 °C)		<i>n</i> -C <sub>10</sub> H <sub>21</sub> –H	130	$8.5 \times 10^{-5}$	$8.7 \times 10^{-4}$	29.5
cyclohexane	27.6 at 25 °C (32.3 at 180 °C)		cyclohexane	180	$<3 \times 10^{-6}$	$<2.8 \times 10^{-5}$	>36.4

<sup>a</sup>  $k_7$  is extrapolated from the reaction scheme indicated (in simplified form) in Scheme 1 (see Table 5 for full details). The value thus obtained (a second-order rate constant) is then multiplied by a statistical factor of 2.0 to allow for unproductive addition/elimination (i.e., elimination of RD, rather than of RH, from the addition product) and multiplied by solvent concentration, to give a pseudo first-order rate constant, rate<sub>7a</sub>. These values are then substituted into the Eyring equation to give free energies of activation for eq 7a, which are directly comparable with the calculated values for C–H addition ( $\Delta G_{4a}^\ddagger$ ).

We estimate a very large error in the determination of these rate constants due to experimental error and possible errors in assumptions concerning isotope effects (see Computational and Experimental Section). Nevertheless, thanks to the generously forgiving nature of logarithms, the final error in the experimental determination of  $\Delta G^\ddagger$  is reasonably small and certainly sufficiently small to provide a useful value for comparison with the calculated data.

H/D exchange with other hydrocarbons, specifically mesitylene-*d*<sub>12</sub> and decane-*d*<sub>22</sub>, requires significantly higher temperatures than C<sub>6</sub>D<sub>6</sub> to achieve conveniently measured rates. The values for the corresponding exchange-reaction rate constants are more easily determined than for C<sub>6</sub>D<sub>6</sub>, because  $k_{RD/IRH}$  is certainly very slow in these cases relative to  $k_{t-Bu/IRH}$ , and the kinetics analysis becomes essentially a one-parameter fit. The resulting rates are shown in Table 3.

Our most significant experimental result regarding H/D exchange is a negative one. Even at 180 °C, cyclohexane-*d*<sub>12</sub> undergoes no observable H/D exchange with ( $^{t-Bu}PCP$ )IrH<sub>2</sub> after 1 week, indicating that addition of cyclohexane-*d*<sub>12</sub> C–D bonds to ( $^{t-Bu}PCP$ )IrH<sub>2</sub> does not occur on this time scale. We can therefore determine a lower limit for the free energy of activation for Cy–H addition to ( $^{t-Bu}PCP$ )IrH<sub>2</sub> (eq 4a) of  $\Delta G^\ddagger > 36.4$  kcal/mol (see Table 3 and accompanying footnote, and Computational and Experimental Section).

The resulting exchange rates for the different hydrocarbons decrease in the following order: phenyl-H > benzyl-H > *n*-alkyl-H > cycloalkyl-H. This trend is familiar in the context of C–H activation, especially by late metal centers. Indeed, to our knowledge, every study involving C–H addition of these substrates has yielded this exact order for both kinetics and thermodynamics.<sup>29,30</sup> Consequently, the relative barriers to H/D exchange are all consistent with the assumption that the exchange rate is a measure of the addition rate of the corresponding C–H bond.

The experimentally determined activation barriers are useful in two distinct respects. First, they provide a comparison with the computational values, and it can be seen from Table 3 that the agreement is quite good although the calculated free energies of activation appear to be slightly too high.<sup>31</sup>

Second, and independent of the good agreement with the calculated values, the experimental values for H/D exchange

fully confirm the major conclusion drawn from the electronic structure calculations reported above (i.e., that the catalytic reaction proceeds via a dissociative pathway), when they are directly compared with *experimentally* measured catalytic rates (Table 4). The catalytic turnover rate is 11 h<sup>-1</sup> ( $3.1 \times 10^{-3}$  s<sup>-1</sup>) for cyclooctane dehydrogenation catalyzed by ( $^{t-Bu}PCP$ )IrH<sub>2</sub> at 151 °C, corresponding to an overall activation barrier of 30.0 kcal/mol. For cyclodecane dehydrogenation, the turnover rate is 90 h<sup>-1</sup> ( $2.5 \times 10^{-2}$  s<sup>-1</sup>) at 201 °C, corresponding to a barrier of 31.7 kcal/mol. The failure of cyclohexane-*d*<sub>12</sub> to undergo any observable H/D exchange with ( $^{t-Bu}PCP$ )IrH<sub>2</sub>, even after 1 week at 180 °C, indicates that the barrier for C–H addition to ( $^{t-Bu}PCP$ )IrH<sub>2</sub> is significantly higher than the experimentally determined barrier to the overall catalytic reaction. Note that cyclohexane has been reported by Bergman to undergo addition *more* readily than cyclooctane, in separate reactions with two different iridium species.<sup>32</sup> Because a catalytic cycle obviously cannot proceed more rapidly than any single step in the cycle, these results are clearly inconsistent with an associative pathway for the catalysis. Or, at the very least, they are inconsistent with the associative pathways calculated in this work by us and calculated by others for smaller substrates,<sup>12</sup> because such pathways are also calculated to lead to H/D exchange. Thus, cycloalkane dehydrogenation must proceed via the **D** pathway with an overall barrier of ca. 31 kcal/mol. The cycloalkane C–H activation step of the **D** pathway can have a barrier no greater than that (though possibly lower). The value for C–H activation of *n*-alkanes is presumably lower still, on the basis of literature precedent for selectivity in C–H activation.<sup>29</sup>

**Considerations on the Remaining Steps of the Full Catalytic Cycle; Relative Rates for Different Alkanes and an Experimental Upper Limit for the Rate of H<sub>2</sub> Loss from (PCP)IrH<sub>2</sub>.** The data in Table 4 reveal that cyclooctane (COA) and cyclodecane are dehydrogenated with significantly lower barriers than *n*-undecane. At first glance, this ordering appears to be inconsistent with *either* the **A** or the **D** pathway. It is opposite that which would be expected from a rate-determining associative reaction, because transition metal complexes add cycloalkane C–H bonds more slowly than primary C–H bonds for all known C–H addition systems.<sup>29</sup> The ordering, however, is also inconsistent with a simple picture involving the dis-

(30) The relative differences in the addition rates among different alkane substrates for kinetic measurements are usually much smaller than those observed in the present case. This is probably because direct measurements of addition rates necessarily involve exothermic additions, whereas in the present case the rate-determining step is endothermic. Thus, the transition state is late and, perhaps more importantly, our kinetic barriers include a thermodynamic barrier. Thermodynamic variations among additions of various hydrocarbons are often found to be of the same order of magnitude as those in the present case.

(31) Most of the currently available functionals (including B3LYP) underestimate intermolecular binding energies and charge-transfer effects at long range. It is possible that the B3LYP functionals differentially overestimate the energies in metal complexes with high coordination numbers and in the transition states, which lead to the formation of these complexes. See, for example: (a) Paizs, B.; Suhai, S. *J. Comput. Chem.* **1998**, *19*, 575. (b) Ruiz, E.; Salahub, D. R.; Vela, A. *J. Am. Chem. Soc.* **1995**, *117*, 1141. (c) Ref 13.

(32) Peterson, T. H.; Golden, J. T.; Bergman, R. G. *J. Am. Chem. Soc.* **2001**, *123*, 455–462.



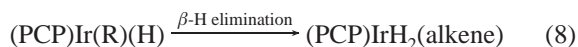
**Table 4.** Experimental Rates for Acceptorless Alkane Dehydrogenation and Corresponding Values of  $\Delta G^\ddagger$ 

catalyst	substrate	$T$ (°C)	rate ( $\text{h}^{-1}$ )	$\Delta G^\ddagger$
( <i>t</i> -BuPCP)Ir	COA	151	11	30.0
( <i>t</i> -BuPCP)Ir	CDA	201	90	31.7
( <i>t</i> -Bu/MeOPCP)Ir <sup>a</sup>	<i>n</i> -C <sub>11</sub> H <sub>24</sub>	196	30	32.4
( <i>i</i> -PrPCP)Ir	COA	151	94	28.2
( <i>i</i> -PrPCP)Ir	CDA	201	400	30.3
( <i>i</i> -PrPCP)Ir	<i>n</i> -C <sub>11</sub> H <sub>24</sub>	196	60	31.7

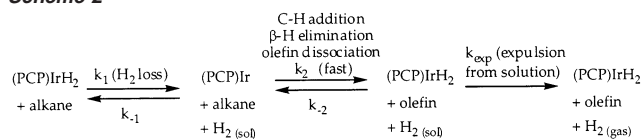
<sup>a</sup> (*t*-Bu/MeOPCP)Ir = [ $\eta^3$ -4-CH<sub>3</sub>O-2,6-[(*t*-Bu<sub>2</sub>P)CH<sub>2</sub>]<sub>2</sub>C<sub>6</sub>H<sub>2</sub>)]Ir.

sociative pathway, if it is assumed that (a) (PCP)IrH<sub>2</sub> is the catalyst resting state (ground state) in all of the reactions and that (b) H<sub>2</sub> loss is irreversible for all of the reactions. On the basis of those two assumptions, the **D** pathway is expected to afford equal rates for all substrates. Thus, it is strongly implied that H<sub>2</sub> loss (regardless of the pathway) is not necessarily irreversible, and subsequent steps in the reaction cycle may, at least in some cases, contribute to the overall reaction barrier. While a detailed characterization of all remaining steps in the cycle is well beyond the scope of this paper, in this section we will briefly consider other steps. In particular, we will consider the one remaining step that the acceptorless system does not have in common with the transfer-dehydrogenation system: the expulsion of H<sub>2</sub> from solution. We believe that consideration of this step is critical in accounting for the apparent discrepancy of the greater reactivity of the cycloalkanes versus *n*-alkanes.

Precise energy barriers for the chemical steps in the catalytic cycle after C–H addition are presently being determined experimentally in the context of transfer-dehydrogenation studies. However, we have previously shown that sources of (*t*-BuPCP)Ir (e.g., (*t*-BuPCP)Ir(Ph)(H)) will readily dehydrogenate alkanes even at 25 °C.<sup>28</sup> We cannot yet experimentally determine the rate of the overall reaction sequence of (*t*-BuPCP)Ir with alkanes, but an upper limit of ca. 18 kcal/mol can be placed on the overall barrier to this sequence (C–H addition, followed by eqs 8 and 9).<sup>9</sup>

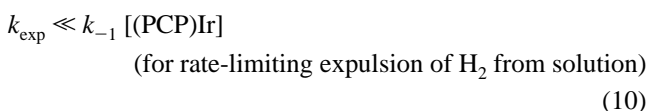


This would imply that C–H addition to (*t*-BuPCP)Ir, as well as  $\beta$ -H elimination and olefin removal, should all proceed more rapidly than the back reaction with H<sub>2</sub> under the conditions required for dehydrogenation (e.g., 150 °C,  $P_{\text{H}_2} \leq \text{ca. } 10^{-7}$  atm). This is in accord with (a) the calculations in this paper, which show the free energy of the C–H addition transition state to be lower than the free energy of the H<sub>2</sub> elimination/addition TS (see Figure 7), and (b) the simple assumption that even if H<sub>2</sub> addition is diffusion controlled ( $k \approx 10^{10} \text{ M}^{-1} \text{ s}^{-1}$ ), the low concentration of H<sub>2</sub> ( $\leq \text{ca. } 10^{-10} \text{ M}$ ) gives a rate of back reaction with H<sub>2</sub> (ca. 1 s<sup>-1</sup>) which is relatively slow (cf., the overall rate of the sequence of C–H addition followed by eqs 8 and 9 is  $\geq 130 \text{ s}^{-1}$  at 150 °C, on the basis of  $\Delta G^\ddagger \leq 21 \text{ kcal/mol}$ ). Hence the loss of H<sub>2</sub> is probably followed by a relatively rapid formation of olefin product for both cyclic and linear alkanes. It must be remembered, however, that the acceptorless dehydrogenation (unlike transfer-dehydrogenation) is an inherently heterogeneous reaction system. If H<sub>2</sub> is not removed sufficiently rapidly from solution, it is possible that the formation of olefin, no matter how rapid, would be reversible.

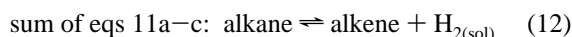
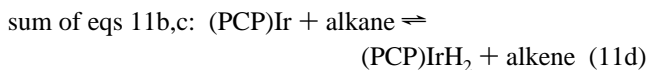
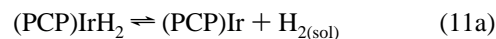
**Scheme 2**

Expressed in terms of Scheme 2,  $k_2[(\text{PCP})\text{Ir}][\text{alkane}]$  appears to be greater than  $k_{-1}[(\text{PCP})\text{Ir}][\text{H}_2(\text{sol})]$ . However, if the rate of expulsion of H<sub>2</sub> from solution,  $k_{\text{exp}}[\text{H}_2(\text{sol})]$ , is less than  $k_{-1}[(\text{PCP})\text{Ir}][\text{H}_2(\text{sol})]$ , the majority of H<sub>2</sub> dissociation events would be ultimately unproductive.

Thus, even assuming that loss of H<sub>2</sub> is rate-determining for the formation of (PCP)Ir(alkyl)(H) (eq 5), as is indicated by the calculations in this paper, it is not necessarily the rate-determining step of the catalytic cycle. Furthermore, even if the loss of H<sub>2</sub> is rate-determining for the overall reaction yielding olefin and H<sub>2</sub> *in solution* (and we believe this to be the case,<sup>9</sup> although it falls outside the scope of the present work), the rate of the catalytic cycle may still be lower than the rate of dissociation of H<sub>2</sub> from (PCP)IrH<sub>2</sub>. This condition would only require that  $k_{\text{exp}}[\text{H}_2(\text{sol})]$  is less than or not much greater than  $k_{-1}[(\text{PCP})\text{Ir}][\text{H}_2(\text{sol})]$ . In the limiting case, which can be expressed as eq 10, expulsion of H<sub>2</sub> from solution could actually be the rate-limiting step.



Under this condition (eq 10), the preequilibria of eqs 11 and 12 would be in effect.



The preequilibrium of eq 11d implies that the concentration of (PCP)Ir would be dependent upon the dehydrogenation thermodynamics of the particular alkane (at a given concentration of alkene). In other words, alkanes with higher dehydrogenation enthalpies (i.e., linear alkanes<sup>24,25</sup>) will result in higher concentrations of (PCP)Ir in solution (eq 11d lies toward the left). The higher concentration of (PCP)Ir results in greater rates of back reaction of H<sub>2</sub> with (PCP)Ir, relative to expulsion of H<sub>2</sub> from solution (i.e., the limit of eq 10 is approached). Thus, the limit of eq 10 should be more readily approached by the buildup of linear alkene product as compared with cycloalkene.<sup>24,25</sup> It is entirely possible, therefore, that the rate-determining step for catalytic dehydrogenation of COA and cyclodecane is loss of H<sub>2</sub> from (PCP)IrH<sub>2</sub>, whereas under similar concentrations and conditions, the rate-limiting step for *n*-alkane dehydrogenation is much more likely to be expulsion of H<sub>2</sub> from solution. This same conclusion may be reached by considering that if reaction 11d proceeds at comparable rates with COA and *n*-alkanes

(which appears to be the case<sup>9</sup>), then the back reaction with linear alkenes is necessarily much faster, because the equilibrium lies much further to the left.

An additional consideration is the possibility that *both* cycloalkane and *n*-alkane systems might operate under preequilibrium (eq 12) conditions. Because this would yield a much greater equilibrium concentration of H<sub>2</sub> for the cycloalkanes,<sup>24,25</sup> the rate of reaction under such conditions,  $k_{\text{exp}}[\text{H}_2(\text{sol})]$ , would be much greater for cycloalkanes. Thus, it is possible that loss of H<sub>2</sub> from (PCP)IrH<sub>2</sub> will be rate-determining for cycloalkanes but not *n*-alkanes or, alternatively, that H<sub>2</sub> expulsion will be rate-determining for both classes of substrates; *in either case, cycloalkanes will give faster rates*. Only in the limit where loss of H<sub>2</sub> from (PCP)Ir is rate-determining for the dehydrogenation of both cycloalkanes and *n*-alkanes ( $k_{\text{exp}} \gg k_{-1}$  [(PCP)Ir]) would equal rates be obtained by the **D** pathway.

Although we have not yet developed methods to monitor the acceptorless dehydrogenation *in situ*, experiments with alkene/alkane mixtures in closed systems strongly indicate that in the case of COA, and probably in the case of *n*-alkanes at low alkene concentration, the resting state is (PCP)IrH<sub>2</sub> at temperatures of 150 °C or greater.<sup>9</sup> The free-energy barrier to the loss of H<sub>2</sub> cannot be greater than the overall catalytic barrier measured for any one of the alkanes. The loss of H<sub>2</sub> (or any other step in the cycle) can have a barrier no greater than the 30.0 kcal/mol found for COA dehydrogenation (cf., the much greater barriers calculated for the **A** pathway). Preliminary kinetic studies of acceptorless COA dehydrogenation indicate that the reaction rate is independent of stirring rate. This would suggest that expulsion of H<sub>2</sub> is highly efficient under these conditions ( $k_{\text{exp}} \gg k_{-1}$  [(PCP)Ir]), specifically with COA as substrate, and that 30.0 kcal is therefore the approximate experimental value of  $\Delta G^\ddagger$  for H<sub>2</sub> loss at 151 °C.<sup>33</sup> Calculations using full bis(*t*-butyl)phosphino groups on the PCP ligand yield a free energy of 27.8 kcal/mol for H<sub>2</sub> addition to (<sup>*t*</sup>-BuPCP)Ir, 0.6 kcal/mol greater than the calculated value for H<sub>2</sub> addition to (<sup>Me</sup>PCP)Ir. The experimental value of 30.0 kcal/mol is in good agreement with this calculated value. Alternatively, if H<sub>2</sub> is in fact *not* removed with a sufficiently high rate under these conditions, that is, if  $k_{\text{exp}}[\text{H}_2(\text{sol})]$  is not much greater than  $k_{-1}[(\text{PCP})\text{Ir}][\text{H}_2(\text{sol})]$  (Scheme 2), then it is possible that dissociation of H<sub>2</sub> (and subsequent alkane dehydrogenation) is occurring reversibly. In this case, the experimental value of 30.0 kcal/mol serves as an experimental upper limit for the barrier to loss of H<sub>2</sub> from (<sup>*t*</sup>-BuPCP)IrH<sub>2</sub>.

In the case of *n*-alkanes, preliminary kinetics data have been less reproducible, but the slower rates indicate that loss of H<sub>2</sub> from (PCP)IrH<sub>2</sub> is not rate-determining. Thus, in accord with the above considerations, the *n*-alkane system may operate under conditions at or approaching the limit in which the preequilibrium of eq 12 is established, and the rate-determining step is expulsion of H<sub>2</sub>. Note that the irreproducibility of the kinetics

is, in itself, consistent with the rate of expulsion of H<sub>2</sub> playing an important role in determining the overall rate. Instrumentation that will allow more quantitative control of the H<sub>2</sub> expulsion rate, which is required for detailed kinetic studies of the system, is currently being designed.

### Summary and Conclusion

Our results may be summarized as follows: The dissociative pathway for the reaction of (<sup>Me</sup>PCP)IrH<sub>2</sub> with alkanes (cyclohexane and propane) is calculated to have an energy barrier ( $\Delta E^\ddagger$ ) of ca. 36 kcal/mol. The highest energy TS for this path involves C–H addition to (<sup>Me</sup>PCP)Ir, after H<sub>2</sub> elimination. For the same pathway,  $\Delta G^\ddagger$  at standard thermodynamic conditions is also ca. 36 kcal/mol, because the entropies of H<sub>2</sub> loss and C–H addition approximately cancel out. However, when the free-energy barriers are calculated for conditions under which dehydrogenation is thermodynamically possible (e.g.,  $T = 150$  °C;  $P_{\text{H}_2} = \text{ca. } 10^{-7}$  atm, with densities of hydrocarbon C–H bonds equal to those in neat solution),  $\Delta G^\ddagger$  for the C–H activation step is much lower, ca. 18 kcal/mol. The large difference is primarily due to the high entropy under these conditions of the free H<sub>2</sub> molecule produced prior to C–H activation. Under these conditions, the rate-determining step is loss of H<sub>2</sub> from (<sup>Me</sup>PCP)IrH<sub>2</sub>, which has an enthalpy (and estimated free energy) barrier of 27.2 kcal/mol (27.8 kcal/mol for (<sup>*t*</sup>-BuPCP)IrH<sub>2</sub>).

An associative pathway for the same reaction is calculated to proceed through Ir(V) and Ir(III)( $\eta^2$ -H<sub>2</sub>) intermediates, in accord with previous calculations on (<sup>H</sup>PCP)IrH<sub>2</sub>.<sup>12</sup> The lowest energy barrier ( $\Delta E^\ddagger$ ) for direct C–H addition to (<sup>Me</sup>PCP)IrH<sub>2</sub> is calculated to be 20.1 kcal/mol (cyclohexane). The loss of H<sub>2</sub> from the resulting manifold of adducts has a higher energy barrier, 28.4 kcal/mol above the level of the reactants. Because there is no barrier calculated for H<sub>2</sub> addition to (<sup>Me</sup>PCP)Ir(R)H,  $\Delta E^\ddagger$  for the overall reaction is equal to  $\Delta E = 28.4$  kcal/mol. At standard thermodynamic conditions, the free-energy barriers for this pathway are much higher:  $\Delta G^\ddagger = 32.2$  kcal/mol for C–H addition and ca. 37.4 kcal/mol for subsequent loss of H<sub>2</sub> from the C–H addition product. Under experimental conditions (e.g.,  $T = 150$  °C;  $P_{\text{H}_2} = \text{ca. } 10^{-7}$  atm, hydrocarbon C–H bond densities equal to those in neat solution), the respective values for C–H addition and H<sub>2</sub> loss are 31.3 and 36.0 kcal/mol for R = Cy (33.7 and 36.6 kcal/mol for R = *n*-Pr).

Consequently, under experimental conditions, the calculated overall free-energy barrier is ca. 9 kcal/mol greater for the **A** pathway. It is further worth noting that even if a TS of lower free energy for the C–H addition step could be located, this would have no bearing on the highest free-energy barrier, the one for the “transition state” for H<sub>2</sub> elimination from the “seven-coordinate” C–H adducts. Because some point on the reaction coordinate must have an enthalpy at least equal to that of the products (25.3 and 24.8 kcal/mol above reactants for R = Cy and *n*-Pr, respectively), and the entropy term ( $T\Delta S$ ) due to the loss of a free hydrocarbon molecule is substantial, especially at higher temperatures, the existence of this very high free-energy barrier for the **A** pathway is unavoidable.<sup>21,34</sup> It should also be noted that the presence of dialkylphosphino groups bulkier than dimethylphosphino would be expected to further increase the free-energy gap favoring the dissociative pathway.

The **A** pathway involves intermediates of the composition (<sup>R</sup>PCP)Ir(alkyl)H<sub>3</sub> which are calculated to undergo rapid

(33) In the case of *n*-alkanes, the slower rates must therefore be attributable to a faster back reaction rehydrogenation of the olefin product as compared with cycloalkenes. Because we have found that *n*-alkanes are dehydrogenated more rapidly than cycloalkanes, and because *n*-alkane dehydrogenation is thermodynamically less favorable, then hydrogenation of linear olefins must indeed be much more rapid than that of cycloalkenes as would be expected in view of both steric and thermodynamic considerations. In terms of Scheme 2,  $k_2[(\text{PCP})\text{IrH}_2][\text{olefin}]$  is apparently greater than  $k_3[\text{H}_2(\text{sol})]$  for linear olefins at the concentrations monitored (> ca. 10 mM), but not for cyclooctene at concentrations in which the stirring rate was varied (< ca. 100 mM).

scrambling among the hydrogen ligands. In the case of deuterated hydrocarbons, this would lead to H/D exchange with  $(^R\text{PCP})\text{IrH}_2$ . Indeed, exchange with  $(^t\text{-BuPCP})\text{IrH}_2$  is observed for several hydrocarbons with rates decreasing in the following order:  $\text{C}_6\text{D}_6 > \text{mesitylene-}d_{12} > n\text{-decane-}d_{10} \gg \text{cyclohexane-}d_{12}$  (cyclohexane- $d_{12}$  does not undergo observable exchange even after 1 week at 180 °C). This order is in agreement with the relative rates calculated for the different hydrocarbons in this work. The absolute free-energy barriers extrapolated for the H/D exchange are also in reasonably good agreement with the calculated barriers, so there is strong evidence that C–H addition to  $(^R\text{PCP})\text{IrH}_2$  can indeed occur along the pathways calculated. However, the barrier to cyclohexane addition (both experimental and computational) is much greater than the experimental barrier to the full catalytic alkane dehydrogenation cycle. Thus, both experimental methods (at least for cycloalkanes) and computational methods (for both propane and cyclohexane) demonstrate that the *A* pathway is not kinetically viable.

The *D* pathway for cycloalkane C–H addition must therefore be operative experimentally with a free-energy barrier no greater than ca. 30 kcal/mol, in good agreement with values calculated for the *D* pathway. For *n*-alkanes, the experimental results alone cannot exclude the *A* pathway. However, the experimental results are consistent with the high barrier to the C–H addition step and certainly not inconsistent with the substantially higher barrier calculated for the subsequent  $\text{H}_2$  elimination. The *D* pathway found for cycloalkanes (with a barrier of ca. 30 kcal/mol) must also be accessible for dehydrogenation of *n*-alkanes; thus all calculated and experimental results are consistent only with the *D* pathway for either cyclic or linear alkanes.<sup>33</sup>

The development of an experimental energy profile for the full catalytic cycle awaits (a) the completion of transfer-dehydrogenation studies, which will yield the precise barriers for C–H addition and  $\beta$ -H elimination steps, and (b) the development of experimental methods suitable for monitoring the reaction in situ and controlling the rate of  $\text{H}_2$  expulsion. However, in the limit where  $\text{H}_2$  is rapidly expelled from solution, the rate-determining step of the catalytic reaction is dissociation of  $\text{H}_2$  from  $(\text{PCP})\text{IrH}_2$ , rather than addition of alkane. This must

be an important consideration in future efforts directed toward rational development of related dehydrogenation catalysts.

## Computational and Experimental Section

**Computational Methods.** All calculations used DFT methodology<sup>35</sup> with Becke's three-parameter hybrid exchange functional (B3) and the Lee–Yang–Parr correlation functional (LYP).<sup>36,37</sup> The Hay–Wadt relativistic, small core ECP and corresponding basis sets (split valence double- $\zeta$ ) were used for the Ir atom (LANL2DZ model).<sup>38</sup> We used all-electron, full double- $\zeta$  plus polarization function basis sets for the second and third row elements C (Dunning–Huzinaga D95(d))<sup>39</sup> and P (McLean–Chandler).<sup>40</sup> Hydrogen atoms in the hydrocarbon, which formally become hydrides in the product complexes, or in dihydrogen were described by the triple- $\zeta$  plus polarization 311G(p) basis set;<sup>41</sup> regular hydrogen atoms in alkyl or aryl groups (including PCP) carried a double- $\zeta$  quality 21G basis set.<sup>42</sup>

Reactant, transition state, and product geometries were fully optimized with the ECP/basis set combination described above (B3LYP/BasisA). The stationary points were characterized further by normal-mode analysis, and the (unscaled) vibrational frequencies formed the basis for the calculation of vibrational zero-point energy (ZPE) corrections. Thermodynamic corrections were made to convert from purely electronic reaction or activation energies ( $\Delta E$ ,  $\Delta E^\ddagger$ ;  $T = 0$  K, no  $\Delta\text{ZPE}$ ) to enthalpies and free energies ( $\Delta H^\circ$ ,  $\Delta H^\circ^\ddagger$ ;  $\Delta G^\circ$ ,  $\Delta G^\circ^\ddagger$ ;  $\Delta\text{ZPE}$  included,  $T = 298$  K,  $P = 1$  atm) according to standard statistical mechanical expressions.<sup>43</sup> Standard techniques were also applied to obtain  $\Delta G$  and  $\Delta G^\ddagger$  at other combinations of temperature and pressure.

Additional single-point calculations at the B3LYP level used a more extended basis set for Ir in which the default LANL2DZ functions for the Ir(6p) orbital were replaced by the functions reoptimized by Couty and Hall,<sup>44</sup> and sets of diffuse d functions (exponent = 0.07) and f functions (exponent = 0.938)<sup>45</sup> were added as well (B3LYP/BasisB). The reoptimized/expanded Ir basis set preferentially favors structures with high Ir coordination numbers.<sup>44,46</sup> All computed energy data discussed in the text or presented in the tables are based on  $\Delta E$  ( $\Delta E^\ddagger$ ) values from these B3LYP/BasisB calculations, followed by electronic energy–enthalpy–free energy conversions (as appropriate) made in an additive fashion with data derived at the B3LYP/BasisA level.

In a few cases, the exact nature of a particular transition state was investigated further by intrinsic reaction coordinate calculations.<sup>47</sup> Approximately 10 steepest descent steps from the transition state were executed in the forward and reverse direction given by the transition vector. The resulting structures were then geometry optimized toward the nearest minimum to assign proper reactants and products.

All calculations were executed using the Gaussian 98 series of computer programs.<sup>48</sup>

**H/D Exchange.**  $(^t\text{-BuPCP})\text{IrH}_2$  was prepared by subjecting  $(^t\text{-BuPCP})\text{IrH}_4$  to vacuum, according to reported methods.<sup>4</sup> Deuterio-

(34) After completion of this work, Haenel, Kaska, and Hall reported an experimental/computational study (ref 13) in which it was concluded that the (anthrphos-PCP)IrH<sub>2</sub> analogue of (PCP)IrH<sub>2</sub> undergoes reaction 5 proceeding through an associative transition state for C–H addition. The computational model used in ref 13 has PH<sub>2</sub> groups in the anthrphos-PCP ligand rather than dimethylphosphino groups (as in our calculations) or bis(*t*-butyl)phosphino groups (as used in both the anthrphos and the PCP-parent experimental systems), and a small model alkane (RH = ethane). Haenel, Kaska, and Hall chose to classify the associative TS as an “interchange TS”. TS<sub>1</sub> was proposed to lead directly to (anthrphos-PCP)IrEtH; that is, C–H cleavage and addition of ethane were concerted with formation and expulsion of H<sub>2</sub>. Some of the computed internuclear distances (Å) in TS<sub>1</sub> are Ir–C<sub>ethyl</sub> (2.176); Ir–H<sub>a</sub> (1.641); C<sub>ethyl</sub>–H<sub>a</sub> (2.58); Ir–H<sub>b</sub> (1.664); Ir–H<sub>c</sub> (1.687); H<sub>b</sub>–H<sub>c</sub> (1.046). Thus, the ethyl carbon and all three hydrogens have normal distances to Ir and show significant bonding with iridium. The C–H distance is 2.58 Å, indicating a fully cleaved C–H bond. Using the exact model species and computational methods applied in ref 13, we have verified the existence and structure of TS<sub>1</sub>. However, graphical examination of the transition vector components for TS<sub>1</sub> shows no structural indications of H<sub>2</sub> expulsion. Rather, the normal mode displacements indicate that TS<sub>1</sub> is a TS for interconversion of two “seven-coordinate” isomers, the analogues of our structures **B** and **C** in Figures 2 and 4. Normal mode following from TS<sub>1</sub> (intrinsic reaction coordinate approach) led cleanly to the intermediate (anthrphos-PCP)IrEtH(H<sub>2</sub>) and (anthrphos-PCP)IrEt(H<sub>2</sub>) species as the “reactant” and “product” connected by TS<sub>1</sub>. In our hands, the proposed rate-limiting TS in ref 13, TS<sub>1</sub>, does not lead to the final products of eq 5, (anthrphos-PCP)IrEtH + H<sub>2</sub>. Also, the energy obtained for TS<sub>1</sub> is peculiar, if TS<sub>1</sub> is associated with a TS leading in a single step from reactants (anthrphos-PCP)IrH<sub>2</sub> + EtH to the (anthrphos-PCP)IrEtH + H<sub>2</sub> products. TS<sub>1</sub> is reported to be approximately 18 kcal/mol lower in enthalpy than these final products (Table 1 of ref 13).

(35) Parr, R. G.; Yang, W. *Density-Functional Theory of Atoms and Molecules*; University Press: Oxford, 1989.

(36) Becke, A. D. *J. Chem. Phys.* **1993**, *98*, 5648–5652.

(37) Lee, C.; Yang, W.; Parr, R. G. *Phys. Rev. B* **1988**, *37*, 785.

(38) Hay, P. J.; Wadt, W. R. *J. Chem. Phys.* **1985**, *82*, 299.

(39) Dunning, T. H.; Hay, P. J. In *Modern Theoretical Chemistry*; Schaefer, H. F., III, Ed.; Plenum: New York, 1976; pp 1–28.

(40) McLean, A. D.; Chandler, G. S. *J. Chem. Phys.* **1980**, *72*, 5639.

(41) Krishnan, R.; Binkley, J. S.; Seeger, R.; Pople, J. A. *J. Chem. Phys.* **1980**, *72*, 650.

(42) Binkley, J. S.; Pople, J. A.; Hehre, W. J. *J. Am. Chem. Soc.* **1980**, *102*, 939.

(43) McQuarrie, D. A. *Statistical Thermodynamics*; Harper and Row: New York, 1973.

(44) Couty, M.; Hall, M. B. *J. Comput. Chem.* **1996**, *17*, 1359.

(45) Ehlers, A. W.; Böhme, M.; Dapprich, S.; Gobbi, A.; Höllwarth, A.; Jonas, V.; Köhler, K. F.; Stegmann, R.; Veldkamp, A.; Frenking, G. *Chem. Phys. Lett.* **1993**, *208*, 111.

(46) If we let  $\Delta\Delta E = \Delta E(\text{B3LYP/BasisB}) - \Delta E(\text{B3LYP/BasisA})$ , we find  $\Delta\Delta E = -3.5$  kcal/mol and  $\Delta\Delta E^\ddagger = -4.8$  kcal/mol for the reaction  $(^M\text{PCP})\text{Ir} + \text{CyH} \rightarrow (^M\text{PCP})\text{Ir}(\text{Cy})(\text{H})$ . For the system  $(^M\text{PCP})\text{IrH}_2 + \text{CyH} \rightarrow (^M\text{PCP})\text{Ir}(\text{Cy})(\text{H})_2$ , we find  $\Delta\Delta E = -3.3$  kcal/mol and  $\Delta\Delta E^\ddagger = -4.8$  kcal/mol.

(47) Gonzalez, C.; Schlegel, H. B. *J. Phys. Chem.* **1990**, *94*, 5523.

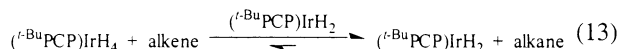
**Table 5.** Complete Set of Reactions and Relative Rate Constants Used for Modeling the Kinetics of H/D Exchange between Deuteriohydrocarbons and (*t*-BuPCP)IrH<sub>2</sub><sup>a</sup>

reaction <sup>b</sup>	rate constant <sup>c</sup>	fixed value (relative) <sup>d</sup>	numerical value (M <sup>-1</sup> s <sup>-1</sup> ) <sup>e</sup>
( <i>t</i> -BuPCP)IrH <sub>2</sub> + RD → ( <i>t</i> -BuPCP)IrHD + RH	<i>k</i> <sub>7</sub>	variable	1.2 × 10 <sup>-4</sup>
( <i>t</i> -BuPCP)IrHD + RH → ( <i>t</i> -BuPCP)IrH <sub>2</sub> + RD	<i>k</i> <sub>-7</sub>	2 × 0.5/ <i>n</i> × <i>k</i> <sub>7</sub>	2.0 × 10 <sup>-5</sup>
( <i>t</i> -BuPCP)IrHD + RD → ( <i>t</i> -BuPCP)IrD <sub>2</sub> + RH	<i>k</i> <sub>2'</sub>	0.5 × <i>k</i> <sub>7</sub>	6.1 × 10 <sup>-5</sup>
( <i>t</i> -BuPCP)IrD <sub>2</sub> + RH → ( <i>t</i> -BuPCP)IrHD + RD	<i>k</i> <sub>-2'</sub>	2/ <i>n</i> × <i>k</i> <sub>7</sub>	4.0 × 10 <sup>-5</sup>
( <i>t</i> -BuPCP)IrH <sub>2</sub> + PD → ( <i>t</i> -BuPCP)IrHD + PH	<i>k</i> <sub>3'</sub>	variable	1.0
( <i>t</i> -BuPCP)IrHD + PH → ( <i>t</i> -BuPCP)IrH <sub>2</sub> + PD	<i>k</i> <sub>-3'</sub>	2 × 0.5 × <i>k</i> <sub>3'</sub>	1.0
( <i>t</i> -BuPCP)IrHD + PD → ( <i>t</i> -BuPCP)IrD <sub>2</sub> + PH	<i>k</i> <sub>4'</sub>	0.5 × <i>k</i> <sub>3'</sub>	5.0 × 10 <sup>-1</sup>
( <i>t</i> -BuPCP)IrD <sub>2</sub> + PH → ( <i>t</i> -BuPCP)IrHD + PD	<i>k</i> <sub>-4'</sub>	2 × 0.5 × <i>k</i> <sub>3'</sub>	2.0
( <i>t</i> -BuPCP)IrH <sub>2</sub> + TD → ( <i>t</i> -BuPCP)IrHD + TH	<i>k</i> <sub>5'</sub>	variable	1.2 × 10 <sup>-1</sup>
( <i>t</i> -BuPCP)IrHD + TH → ( <i>t</i> -BuPCP)IrH <sub>2</sub> + TD	<i>k</i> <sub>-5'</sub>	0.5 × <i>k</i> <sub>-5'</sub>	6 × 10 <sup>-2</sup>
( <i>t</i> -BuPCP)IrHD + TD → ( <i>t</i> -BuPCP)IrD <sub>2</sub> + TH	<i>k</i> <sub>6'</sub>	0.5 × <i>k</i> <sub>-5'</sub>	6 × 10 <sup>-2</sup>
( <i>t</i> -BuPCP)IrD <sub>2</sub> + TH → ( <i>t</i> -BuPCP)IrHD + TD	<i>k</i> <sub>-6'</sub>	1.0 × <i>k</i> <sub>-5'</sub>	1.2 × 10 <sup>-1</sup>

<sup>a</sup> Numerical values determined for C<sub>6</sub>D<sub>6</sub> are given; values for *k*<sub>7</sub> given in Table 4 for other deuteriohydrocarbons. <sup>b</sup> RD = deuteriohydrocarbons; PH(D) = PCP *tert*-butyl hydrogens (deuterons); TH(D) = hydrides (deuterides) of (*t*-BuPCP)IrH<sub>2</sub>D<sub>4-*x*</sub>. <sup>c</sup> *k*<sub>7</sub> and *k*<sub>-7</sub> refer to eq 7. Other rate constants do not correspond to equations in the text and are indicated as *k*<sub>*n*'</sub>. <sup>d</sup> *n* = statistical correction for number of H's in RH (actually monoprotonated deuteriohydrocarbon) as compared with number of equivalent D's in RD, for example, *n* = 6 for reactions with C<sub>6</sub>D<sub>6</sub>. <sup>e</sup> Numerical values for RD = C<sub>6</sub>D<sub>6</sub>; for other deuteriohydrocarbons, *k*<sub>3'</sub> and *k*<sub>5'</sub> were set to an arbitrary high value relative to *k*<sub>7</sub> (1.0 s<sup>-1</sup>; see Table 4 for other values obtained for *k*<sub>7</sub>).

hydrocarbon solvents were distilled from Na/K alloy. Solutions of ca. 0.030 M (*t*-BuPCP)IrH<sub>2</sub> were prepared and transferred to an NMR tube which was then flame-sealed.

Because our interest was specifically in determining the rate of C–H addition to (*t*-BuPCP)IrH<sub>2</sub>, it was desirable to disfavor any other pathways that might potentially lead to H/D exchange. In particular, in the case of alkanes, there was concern that a degenerate transfer-hydrogenation/dehydrogenation involving even trace amounts of corresponding alkene could lead to rapid H/D exchange without proceeding via reaction 4a. To minimize this possibility, all runs were conducted with small amounts of (*t*-BuPCP)IrH<sub>4</sub> present (ca. 2–5 mol %). This was obtained simply by *not* driving the conversion from (*t*-BuPCP)IrH<sub>4</sub> to (*t*-BuPCP)IrH<sub>2</sub> to completion. Our hope was that the presence of (*t*-BuPCP)IrH<sub>4</sub> would keep the steady-state alkene concentration to an absolute minimum. Because (*t*-BuPCP)IrH<sub>4</sub> loses free H<sub>2</sub>, the thermodynamics of alkene hydrogenation must be very favorable and lie very far to the right:



We still cannot exclude the possibility that transfer-hydrogenation/dehydrogenation or other undesired H/D exchange pathways were in fact operative to at least a partial extent. However, because we use the observed H/D exchange rates to obtain upper limits for the rate of eq 4, any such pathways would not invalidate the conclusions obtained from this work.

The total concentration of dihydride and tetrahydride was found to remain unchanged during the kinetic runs, as determined by <sup>1</sup>H NMR observation of the PCP methylene protons ((*t*-BuPCP-*d*<sub>*n*</sub>)IrH<sub>2</sub>: δ –3.47(vt), *J*<sub>PH</sub> = 6.4 Hz, dihydride; (*t*-BuPCP-*d*<sub>*n*</sub>)IrH<sub>4</sub>: 3.24(vt), *J*<sub>PH</sub> = 3.4 Hz) and an external (capillary) standard. <sup>1</sup>H NMR was also used to monitor (a) the total concentration of iridium dihydride, (*t*-BuPCP-*d*<sub>*n*</sub>)IrH<sub>2</sub> (δ –19.194(t), *J*<sub>PH</sub> = 8.7 Hz; *n* = 0–36); (b) the total concentration of hydridodeuteride, (*t*-BuPCP-*d*<sub>*n*</sub>)IrHD (δ –19.039(t), *J*<sub>PH</sub> = 8.4 Hz; *n* = 0–36); (c) the fraction of deuteration of the total *t*-BuPCP *tert*-butyl hydrogens (δ 1.22(vt) *J*<sub>PH</sub> = 6.4 Hz); (d) the fraction of deuteration of the total (*t*-BuPCP-*d*<sub>*n*</sub>)IrH<sub>*m*</sub>D<sub>(4-*m*)</sub> (tetrahydride) hydrides (δ –9.48(t) *J*<sub>PH</sub> = 9.8 Hz); and (e) the fraction of protiation of the deuteriohydrocarbon. Thus, a total of five different experimental parameters were measured.

The concentrations of all species were fit to the reaction scheme indicated in Table 5.

At the outset of this discussion, it is important to note that we required only a value for *k*<sub>7</sub>, and that value was needed at only a very approximate level. Ultimately, the data fits were shown to be highly insensitive to the other variables and therefore essentially amounted to

fits based on one parameter, *k*<sub>7</sub> (see below). This allows a higher level of certainty in *k*<sub>7</sub> than if the fits were also sensitive to other parameters. We believe that our results, for *k*<sub>7</sub>, have an uncertainty of less than ±25%; this corresponds to an uncertainty in Δ*G*<sup>‡</sup> of ±0.2 kcal/mol (even a factor of 2.0 corresponds to an acceptable error level of only ±0.4 kcal/mol at 30 °C).

The kinetics modeling scheme treated the PCP *t*-butyl hydrogens (deuterons) as a pool of individual species with a total “concentration” 36 times that of total iridium. This was consistent with our experimental method, which could only determine the fraction of total PCP *t*-butyl deuteration, and this obviated the need to treat each of the 36 possible isotopomers separately for kinetics modeling. A pseudo second-order rate constant, *k*<sub>3'</sub>, for exchange between the hydrides and *tert*-butyl hydrogen is then obtained; this value is not physically meaningful, assuming that the exchange is intramolecular, but it allows us to extrapolate *k*<sub>7</sub>. In principle, a physically meaningful first-order rate constant for exchange could be obtained by multiplying *k*<sub>3'</sub> by (36 × [(*t*-BuPCP)IrH<sub>2</sub>-*d*<sub>*n*</sub>]). However, as this value was not directly relevant to this work, such a conversion to first-order was unnecessary, and because the reaction in all cases was fast relative to *k*<sub>7</sub>, it could, in any case, only serve as a very approximate lower limit. The hydrides/deuteride ligands of (*t*-BuPCP)IrH<sub>4</sub>-*d*<sub>*n*</sub> were similarly treated as a pool of individual species. Unlike the hydrides/deuterides of (*t*-BuPCP-*d*<sub>*n*</sub>)IrH<sub>2</sub>-*d*<sub>*n*</sub>, the various isotopomers of (*t*-BuPCP)IrH<sub>4</sub>-*d*<sub>*n*</sub> could not be resolved by <sup>1</sup>H NMR.

Rate constants *k*<sub>-7</sub>, *k*<sub>2'</sub>, and *k*<sub>-2'</sub> are chemically equivalent to *k*<sub>7</sub>. *k*<sub>2'</sub> was set equal to 0.5 × *k*<sub>7</sub> because it was assumed that statistically the rate of RD exchange with (*t*-BuPCP)IrHD would be one-half the rate with (*t*-BuPCP)IrH<sub>2</sub>. Likewise, *k*<sub>-7</sub> was set equal to 0.5 × *k*<sub>-2'</sub>. Both rate constants contained the statistical term, 1/*n*, where *n* is the number of chemically equivalent H's in the perproteo-hydrocarbon, to account for the fact that the RH product was only monoprotonated (e.g., C<sub>6</sub>D<sub>5</sub>H where *n* = 6).

Although kinetic isotope effects for C–H activation reactions vary greatly, equilibrium isotope effects vary much less so because the relevant vibrational frequencies of the respective ground states are far

- (48) Frisch, M. J.; Trucks, G. W.; Schlegel, H. B.; Scuseria, G. E.; Robb, M. A.; Cheeseman, J. R.; Zakrzewski, V. G.; Montgomery, J. A., Jr.; Stratmann, R. E.; Burant, J. C.; Dapprich, S.; Millam, J. M.; Daniels, A. D.; Kudin, K. N.; Strain, M. C.; Farkas, O.; Tomasi, J.; Barone, V.; Cossi, M.; Cammi, R.; Mennucci, B.; Pomelli, C.; Adamo, C.; Clifford, S.; Ochterski, J.; Petersson, G. A.; Ayala, P. Y.; Cui, Q.; Morokuma, K.; Malick, D. K.; Rabuck, A. D.; Raghavachari, K.; Foresman, J. B.; Cioslowski, J.; Ortiz, J. V.; Baboul, A. G.; Stefanov, B. B.; Liu, G.; Liashenko, A.; Piskorz, P.; Komaromi, I.; Gomperts, R.; Martin, R. L.; Fox, D. J.; Keith, T.; Al-Laham, M. A.; Peng, C. Y.; Nanayakkara, A.; Gonzalez, C.; Challacombe, M.; Gill, P. M. W.; Johnson, B.; Chen, W.; Wong, M. W.; Andres, J. L.; Gonzalez, C.; Head-Gordon, M.; Replogle, E. S.; Pople, J. A. *Gaussian* 98, revision A.9; Gaussian, Inc.: Pittsburgh, PA, 1998.

more constant in value than those of the transition states. For the sake of simplicity, we kept the same ratio, 2.0, for all reactions involving transfer of H/D from C to Ir (e.g.,  $k_7/k_{-7}$  or  $k_3/k_{-3}$ ). This somewhat arbitrary value was obtained by taking a well-determined equilibrium isotope effect for C–H addition, 2.4 for addition to TpRh(CN-neopentyl)<sup>49</sup> at 26 °C, and extrapolating to the midpoint of the temperature range most relevant to this work (30–180 °C). The final value of  $k_7$  was not very sensitive to the value used (e.g., an assumed isotope effect of 1.4 gave values within 10% of those obtained using 2.0). It was assumed that there was no significant equilibrium isotope effect in the exchange between dihydride and tetrahydride.

The reactions were monitored at intervals of ca. 2000 s. Data for benzene and *n*-decane (experimental and least-squares best-fit calculated) are given in the Supporting Information. Benzene gave the best data probably because the low temperature of the reaction, 30 °C, allowed continuous heating in the NMR spectrometer, whereas other samples had to be removed, heated, and then returned to the spectrometer. The resulting fit was found to be highly insensitive to the values for variables  $k_{3'}$  and  $k_{5'}$  because these rates were rapid relative to  $k_7$ . The sum of the squares of the differences ( $\sum(\text{exp} - \text{calc})^2$ ) decreased asymptotically with increasing values of  $k_{3'}$  (exchange between *t*-butyls and hydrides).

The factors used for  $k_{-7}$  and  $k_{-2'}$  were also unimportant in optimizing the fit, because the corresponding rates were slow due to the very low concentrations of RH (particularly after correction for the statistical term,  $n$ , which is required because the “RH” product is only mono-proteated RD). Thus, the kinetics simulation was essentially a fit to the one parameter of interest,  $k_7$ . This conclusion was even more applicable to the other deuteriohydrocarbons, because the corresponding values of  $k_7$  were much smaller, relative to presumed values of  $k_{3'}$  and  $k_{5'}$  at the much higher temperatures used for these substrates.

Using a macro written for Microsoft Excel 98 for Macintosh, we calculated the concentrations of each species at small finite time intervals (0.5 s) using the appropriate kinetic equation. For example,

for (<sup>*t*</sup>-BuPCP)IrH<sub>2</sub>:

$$n\text{IrH}_2 = \text{IrH}_2 + (-k_7 * \text{IrH}_2 * \text{RD} - k_3 * \text{IrH}_2 * \text{PD} + k_{-7} * \text{IrHD} * \text{RH} + k_{-3} * \text{IrHD} * \text{PH} - k_5 * \text{IrH}_2 * \text{TD} + k_{-5} * \text{IrHD} * \text{TH}) dt$$

IrH<sub>2</sub> is [(<sup>*t*</sup>-BuPCP)IrH<sub>2</sub>] at the outset of each time interval,  $dt$ ;  $n\text{IrH}_2$  is the resulting concentration at the end of each time interval (other abbreviations are defined in footnote *a*, Table 5). The use of time intervals smaller than 0.5 s had no effect on the concentrations that were calculated for the experimental times (ca. every 2000 s). Rate constants were then calculated by iterating to minimize the sums of the squares ( $\sum[(\text{exp} - \text{calc})^2/\text{exp}_{\text{avg}}]$ ), weighted for the time-averaged concentrations of various species that were monitored. It was established by iteration of  $k_3$ ,  $k_5$ , and  $k_7$  that  $k_{3'}$  and  $k_{5'}$  were large relative to  $k_7$  for benzene (Table 5). For other deuteriohydrocarbons, where  $k_7$  was smaller and temperatures were much higher, it was assumed that  $k_{3'}$  and  $k_{5'}$  were large relative to  $k_7$ . Thus,  $k_{3'}$  and  $k_{5'}$  were set at an arbitrary high value (1.0 s<sup>-1</sup>) for other deuteriohydrocarbons, and it was subsequently confirmed that varying  $k_{3'}$  and  $k_{5'}$  in that regime had no effect on the calculated fit. Raw data and corresponding calculated data points are given in the Supporting Information for the exchange reactions with C<sub>6</sub>D<sub>6</sub> and *n*-C<sub>10</sub>D<sub>22</sub>, respectively.

**Acknowledgment.** We thank the Division of Chemical Sciences, Office of Basic Energy Sciences, Office of Energy Research, U.S. Department of Energy for support of this work, and the National Science Foundation for a computer equipment grant (DBI-9601851-ARI).

**Supporting Information Available:** Data (concentrations determined by <sup>1</sup>H NMR) used to obtain (least-squares best-fit) rate constants for H/D exchange between deuteriohydrocarbons (C<sub>6</sub>D<sub>6</sub> and *n*-decane-*d*<sub>22</sub>) and (<sup>*t*</sup>-BuPCP)IrH<sub>2</sub> and corresponding calculated values (PDF). This material is available free of charge via the Internet at <http://pubs.acs.org>.

(49) Northcutt, T. O.; Wick, D. D.; Vetter, A. J.; Jones, W. D. *J. Am. Chem. Soc.* **2001**, *123*, 7257–7270.